Dual influence of terrestrial and marine historical processes on the phylogeography of the Brazilian intertidal red alga Gracilaria caudata

Lígia Ayres-Ostrock, Myriam Valero, Stéphane Mauger, Mariana C Oliveira, Estela M Plastino, Marie-Laure Guillemin, Christophe Destombe

Dual influence of terrestrial and marine historical processes on the phylogeography of the Brazilian intertidal red alga *Gracilaria caudata*[1]

Lígia M. Ayres-Ostrock, Instituto de Biociências, Universidade de São Paulo, Rua do Matão 277, CEP: 05508-090 São Paulo, SP, Brazil.

Myriam Valero, CNRS, Sorbonne Université, UMI 3614, Evolutionary Biology and Ecology of Algae, Station Biologique de Roscoff, CS 90074, 29688 Roscoff, France;

Stéphane Mauger, CNRS, Sorbonne Université, UMI 3614, Evolutionary Biology and Ecology of Algae, Station Biologique de Roscoff, CS 90074, 29688 Roscoff, France;

Mariana C. Oliveira, Instituto de Biociências, Universidade de São Paulo, Rua do Matão 277, CEP: 05508-090 São Paulo, SP, Brazil;

Estela M. Plastino[2], Instituto de Biociências, Universidade de São Paulo, Rua do Matão 277, CEP: 05508-090 São Paulo, SP, Brazil; emplasti@usp.br, phone/fax: +55(11) 3091-7544;

Marie-Laure Guillemin, CNRS, Sorbonne Université, UMI 3614, Evolutionary Biology and Ecology of Algae, Station Biologique de Roscoff, CS 90074, 29688 Roscoff, France; Instituto de Ciencias Ambientales y Evolutivas, Facultad de Ciencias, Universidad Austral de Chile, Valdivia, Chile;

Christophe Destombe, CNRS, Sorbonne Université, UMI 3614, Evolutionary Biology and Ecology of Algae, Station Biologique de Roscoff, CS 90074, 29688 Roscoff, France.

Condensed running title: PHYLOGEOGRAPHY OF *G. CAUDATA*

ABSTRACT

In this study, we explored how both past terrestrial and marine climate changes have interacted to shape the phylogeographic patterns of the intertidal red seaweed *Gracilaria caudata*, an economically important species exploited for agar production in the Brazilian north-east. Seven sites were sampled along the north-east tropical and south-east sub-tropical Brazilian coast. The genetic diversity and structure of *G. caudata* was inferred using a combination of mitochondrial (COI and *cox*2-3), chloroplast (*rbc*L) and 15 nuclear microsatellite markers. A remarkable congruence between nuclear, mitochondrial and chloroplast data revealed clear separation between the north-east (from 03°S to 08°S) and the south-east (from 20°S to 23°S) coast of Brazil. These two clades differ in their demographic histories, with signatures of recent demographic expansions in the north-east and divergent populations in the south-east, suggesting the maintenance of several refugia during the last glacial maximum due to sea-level rise and fall. The Bahia region (around 12^{o}S) occupies an intermediate position between both clades. Microsatellites and mtDNA markers showed additional levels of genetic structure within each sampled site located south of Bahia. The separation between the two main groups in *G. caudata* is likely recent, probably occurring during the Quaternary glacial cycles. The genetic breaks are concordant with (1) those separating terrestrial refugia, (2) major river outflows and (3) frontiers between tropical and subtropical regions. Taken together with previously published eco-physiological studies that showed differences in the physiological performance of the strains from distinct locations, these results suggest that the divergent clades in *G. caudata* correspond to distinct ecotypes in the process of incipient speciation and thus should be considered for the management policy of this commercially important species.

KEYWORDS

55 COI mtDNA, *Gracilaria caudata*, microsatellite, phylogeography, population genetics, refugia,
56 Rhodophyta, South-western Atlantic Coast.

57

58 LIST OF ABBREVIATIONS

59

60 AMOVA: analysis of molecular variance

61 AR: allelic richness

62 BA: Bahia

63 BC: Brazil Current

64 CE: Ceará

65 COI: cytochrome c oxidase I gene

66 *cox*2-3: intergenic spacer located between the cytochrome oxidase subunits 2 and 3 genes

67 DAPC: discriminant analysis of principal components

68 ES: Espírito Santo

69 F_{IS}: single- and multi-locus estimates of deviation from random mating

70 F_{ST}: genetic differentiation between sites

71 H: gene diversity

72 h: the number of haplotypes

73 H_e: expected heterozygosity

74 H_o: observed heterozygosity

75 K: clusters

76 LD: Linkage disequilibrium

77 LGM: Last Glacial Maximum

78 MAAs: mycosporine-like amino acids

79 ML: Maximum likelihood

N_a: mean number of alleles per locus

NBC: North Brazil Current

NE: north-eastern

PB: Paraíba

PE: Pernambuco

R: clonal richness

*rbc*L: large subunit of ribulose-l, 5-bisphosphate carboxylase/oxygenase

RN: Rio Grande do Norte

S: number of polymorphic sites

SACW: South Atlantic Central Waters.

SE: south-eastern

SEC: South Equatorial Current

SP: São Paulo

π: nucleotide diversity

INTRODUCTION

Historical processes have likely influenced hydrographic-climatic patterns, in addition to modifying coastline profiles and marine species' range dynamics (Haq et al. 1987, Hewitt 1996, 2000, 2004). Likewise, these processes may have shaped genetic diversity: the genetic structure of contemporary populations is the result of both short-term ecological processes and long-term evolution governed in part by environmental changes (Benzie 1998). Phylogeographic approaches, generally using uniparentally inherited molecular markers, are powerful tools for inferring past range contraction and expansion and to establish evolutionary origin of genetic characteristics of present-day populations (Avise 2000). The late Pleistocene glaciations are recognised as important factors that favoured the divergence of populations and ultimately speciation via repeated isolation in allopatric refuges (Hewitt 1996, 2004, Maggs et al. 2008, Neiva et al. 2016, Bringloe and Saunders 2018). After the Last Glacial Maximum (LGM), it is assumed that climatic amelioration allowed species to expand their range poleward from the populations located at low latitude margins (Davis and Shaw 2001). Thus, current patterns of genetic diversity have been largely determined by population responses at the margins of species' distribution ranges (Hampe and Petit 2005). Long-term persistent populations, also known as 'rear-edge' populations, are usually restricted to areas where survival was possible under glacial maximum conditions. These low-latitude refugia show generally high genetic variation despite bottlenecks in these isolated populations during glacial periods (Hewitt 1996, 2004, Assis et al. 2016). On the other hand, 'leading-edge' populations result from rare long-distance dispersal events followed by exponential population growth and are generally characterised by highly reduced genetic diversity (Hewitt 2000).

In tropical and sub-tropical zones, the effect of glacial-interglacial cycles was less dramatic than in temperate ones and changes in species distribution, mostly related to a cooler and more arid climate during glacial periods, generally do not reflect the classical contraction and expansion

reported at higher latitudes (Lessa et al. 2003). In Brazil, phylogeographic studies have mainly focused on terrestrial and freshwater habitats (e.g. Costa et al. 2003, Rocha 2003, Carnaval and Moritz 2008), whereas marine organisms have received little attention (Pinheiro et al. 2017, Nauer et al. 2019). Nonetheless, studies on marine population genetics are crucial to assure a better sustainable management and future economic stability of these natural resources (Palumbi 2003, Waples et al. 2008, Couceiro et al. 2013).

The Brazilian coast extends for about 8000 km and stretches across 38 degrees of latitude (from 5°16'20"N to 33°44'32"S, Figure 1). This long coastline provides a variety of ecological conditions resulting in very different abiotic environments (Gomes da Silva et al. 2016). Phylogeographic patterns in marine fishes and invertebrates are generally more related to the impact of the strong currents affecting the region and acting as barriers to gene flow (e.g., the bifurcation into two branches of the South Equatorial Current at latitudes 10º-15ºS; see Figure 1; Santos et al. 2006, da Silva Cortinhas et al. 2016, dos Santos Freitas et al. 2017, Peluso et al. 2018) than to demographic processes linked to Pleistocene climatic changes. Interestingly, intertidal species such as some seaweeds located at the interface of the terrestrial and marine realms may have been affected by past marine and terrestrial climatic fluctuations (Neiva et al. 2014, Cardoso et al. 2015). The existence of three main refugia for the rainforest located along the Brazilian Atlantic coast have been postulated (i.e. in the region of Pernambuco-PE, Bahia-BA, and São Paulo-SP, Figure 1) for which long term persistence of genetically isolated lineages have been associated (Carnaval and Moritz 2008, Carnaval et al. 2009). Additionally, along the Brazilian coast, the Holocene sea-level history suggests regional variations alternating periods of mean sea-level rise and fall. It may be assumed that these oscillations would have had a strong influence on the distribution and diversity of coastal species (Cardoso et al. 2015, Leite et al. 2016).

Phylogeographic studies on seaweeds have increased significantly over the past two decades (for review see Hu et al. 2016). Most of these studies have been carried out in the Northern

Hemisphere and only a few have focused on South America (Tellier et al. 2009, 2011, Guillemin et al. 2016, 2018, Montecinos et al. 2012). Recently, Nauer et al. (2015, 2019) highlighted the existence of intraspecific diversity within the intertidal red alga *Hypnea pseudomusciformis* along the Brazilian coast, with divergence between samples from the north-central part of the distribution and the ones located on the more south-eastern part of the coast. Here, we report on the phylogeographic patterns of the intertidal red alga *Gracilaria caudata*. The order Gracilariales a taxonomically challenging group of marine benthic red algae, includes species of major ecological and economical importance (worldwide invasive species: Bellorin et al. 2004, Krueger-Hadfield et al. 2016; harvested and cultivated agarophyte species: Valero et al. 2017). . Morphological species delineation is particularly difficult due to the relatively small number of diagnostic characters and their great phenotypic plasticity (Gurguel et al. 2004). Recent molecular-based analyses revealed the occurrence of numerous cryptic species in this group (Cohen et al. 2004, Guillemin et al. 2008, Destombe et al. 2010, Lyra et al. 2016). The difficulty in distinguishing species also explains the current debate about the classification of the Gracilariales (see Gurgel et al. 2018 and Iha et al. 2018). *Gracilaria caudata* is a haploid-diploid intertidal rocky shore species characterized by forming dense beds. The species is widespread and occurs from southern Florida (USA-27°N) to the southern part of the Brazilian coast (Santa Catarina State, SC-27^{o}S; Plastino and Oliveira 1997). This species is an important source of agar production in Brazil (Hayashi et al. 2014). Over the last 50 years, intensive and uncontrolled exploitation of natural beds has led to a significant decline of native populations (Hayashi et al. 2014). Today, artisanal mariculture of *G. caudata* in the north-east State of Ceará, Brazil offers an important source of income for the local fishing community (Costa et al. 2012). Over the past two decades, the taxonomy, physiology, ecology, life history and mariculture of this species of economic interest have been intensively studied (Plastino and Oliveira 1997, Costa et al. 2012, Araújo et al. 2014; Faria and Plastino 2016, Faria et al. 2017, Trigueiro et al. 2017). Recently, a comparative study of individuals from three distant geographical areas along the Brazilian coast done

under laboratory conditions, showed clear differences in the physiological performance of *G. caudata* strains among regions with strains from the north-east state of Ceará (CE) presenting higher growth rates and better photosynthetic performances than the ones sampled in the south (BA and SP) (Faria et al. 2017). Moreover, differences in growth rate and sensitivity to UVB radiation were observed between strains from CE and SP under controlled laboratory conditions (Araújo et al. 2014). These differences suggest the existence of intraspecific diversity, supporting the hypothesis of ecotypic differentiation within this species (Araújo et al. 2014, Faria et al. 2017), and raising questions on gene flow patterns and possible reproductive isolation along the extensive range of *G. caudata*. These results are also critical for developing effective management strategies in priority areas for conservation of coastal and marine biodiversity in Brazil (Prates et al. 2007).

Using mitochondrial and chloroplast DNA sequences and nuclear microsatellite markers, we examine the population genetic structure of *G. caudata* throughout its whole distribution range in Brazil. We use this combined information to test for 1) the existence of differentiated genetic groups that echo the ecotypic differences revealed by eco-physiological experiments and 2) the processes responsible for population structuring. We hypothesised that both past isolation in refugia and oceanic barriers to gene flow have affected genetic structuring of *G. caudata* and that the main barriers to gene flow coincide with previously reported biogeographical breaks in the South-West Atlantic and/or with strong marine circulation patterns.

MATERIAL AND METHODS

Study Species

Gracilaria caudata is a commonly encountered seaweed in Brazil. The species grows on rocky substrate, often partially buried in sand and forming dense beds. It occurs mostly in protected bays and turbid waters, extending from the intertidal to the subtidal fringe (Plastino and Oliveira 1997). In

Gracilaria, the tetrasporophytic, female gametophytic and male gametophytic individuals are isomorphic. The thallus is an erect system of cylindrical branches that grow from the holdfast, fixing the individual to the substrate. Male and tetrasporophytic individuals can be distinguished by their reproductive structures, which are readily visible under a dissecting microscope, while female individuals are recognized by the presence of cystocarps (when fertilized) and can be detected by direct observation. In *Gracilaria*, as in most red algae, none of the propagules released in the seawater during the sexual life cycle (i.e, spermatia, haploid and diploids spores) are motile (Kain and Destombe 1995) and even if thalli are detached and found washed up on beach, they are not buoyant. As expected, gene flow has been estimated to be generally restricted to a few meter or kilometer in these algae (Engel et al. 1999, 2004, Guillemin et al. 2008); but in Guillemin et al. (2014) an event of rare long-distance dispersal caused by trans-oceanic colonization of non-buoyant algae species in association with rafting seaweeds is suggested for *G. chilensis*.

Sample collection

A total of 735 individuals of *G. caudata* were randomly collected from seven sites (Figure 1) covering most of the species' distribution range along the Brazilian coast including priority areas for conservation of coastal and marine biodiversity in Brazil (Prates et al. 2007). Two sampling strategies were adopted depending on algal density and spatial distribution. When possible (i.e. in CE, RN, PB, PE and BA), three transects of 20 meters in length were done perpendicularly to the shoreline during the low tide. For each transect, the apical branches of 35 individuals were sampled, resulting in 105 per site site. At sites with low densities of *G. caudata* (i.e. ES and SP), the sampling was done randomly and at least 50 individuals were collected. Each sample corresponds to an individual holdfast. All specimens were collected in between high and low intertidal areas uncovered at low tide.

Life stage and sex of individuals were determined by reproductive structures (by eyes for fertilized females or under a stereoscopic microscope for males and tetrasporophytes).Only diploid individuals (a total of 411 samples, i.e. more than 50 individuals per site) were preserved for genotyping. For the phylogeographic study, a subsampled of 18 tetrasporophytic individuals per site were sequenced.

DNA extraction and PCR amplification of mitochondrial, chloroplast and nuclear microsatellite markers

DNA extractions followed the procedures described in Ayres-Ostrock et al. (2016). PCR amplifications of the mitochondrial cytochrome *c* oxidase I gene (COI) and the intergenic spacer located between the cytochrome oxidase subunits 2 and 3 genes (*cox*2-3) were performed following the protocols described in Saunders (2005) and Zuccarello et al. (1999). To supplement the mitochondrial marker data set, some individuals were sequenced for the chloroplast gene for the large subunit of ribulose-l, 5-bisphosphate carboxylase/oxygenase (*rbc*L). PCR amplifications were carried out following the protocol described in Freshwater et al. (1994).

All PCR products were purified using Illustra™ GFX™ MicroSpin™ columns (GE Healthcare, Chicago, USA) and sequenced using the BigDye™ Terminator v3.1 Cycle Sequencing kit (Thermo Fisher Scientific, Waltham, USA), with the forward and the reverse amplification primers. PCR amplifications and genotyping of the 15 microsatellite loci were performed according to Ayres-Ostrock et al. (2016).

Mitochondrial and chloroplast DNA markers: sequence alignment, phylogenetic reconstructions, diversity and network analyses

Sequences were edited and aligned using ClustalW/Bioedit v 7 (Hall, 1999) and Mega v 5 (Tamura et al. 2011) and deposited in GenBank under accession numbers MF995393-MF995549 for COI, MG452409-MG452552 for *cox*2-3 and MF995550-MF995561 for *rbc*L.

Maximum likelihood (ML) phylogenetic trees were constructed independently for *rbc*L and for the concatenated sequences of the two mitochondrial markers (COI and *cox*2-3) with Iq-Tree software using 2000 iterations for the optimal-tree search and as bootstrap pseudo-replicates (Minh et al. 2013, Nguyen et al. 2014, Kalyaanamoorthy et al. 2017). Phylogenetic trees were visualised in Figtree v1.4.3 (http://tree.bio.ed.ac.uk/software/figtree/). For *rbc*L, four sequences of *G. secunda* and eight of *G. caudata* from the USA, Mexico, Venezuela and Brazil were downloaded from GenBank and added to our data set. For both trees, *G. birdiae* was used as outgroup. Moreover, a haplotype network was reconstructed for the concatenated COI+*cox*2-3 dataset using the median-joining algorithm implemented in Network v 5.0.0.1 (Bandelt et al. 1999).

Pairwise values of F_{ST} among locations were calculated and their significance was tested using 1000 permutations. Moreover, a nested analysis of molecular variance (AMOVA) was implemented to test for the partition of genetic variance within sites, between sites within haplogroups and among haplogroups (Excoffier et al. 1992). The isolation-by-distance model (Mantel test) was used to test for a relationship between genetic distance (F_{ST}) and geographic distance (in km), and its significance was tested using 1000 permutations.

For each site, four diversity indices were calculated for the COI and *cox*2-3 markers using Arlequin: the number of haplotypes (h), the number of polymorphic sites (S), gene diversity (H) (Nei, 1987) and nucleotide diversity (π) (Nei and Li, 1979). A Mann-Whitney U test was used to evaluate differences in genetic diversity among regions (north-east vs. south-east) using Statistica 10 software.

Microsatellite scoring, diversity within sites and structuration patterns

For the 15 microsatellite loci, allele size was scored manually according to Ayres-Ostrock et al. (2016). Initially, the frequency of null alleles was estimated using MICRO-CHECKER software (van Oosterhout et al. 2004). The frequency of different multi-locus genotypes was calculated using the Monte Carlo procedure implemented in GenClone 2.0 (Arnaud-Haond and Belkhir 2007). Genotype diversity was calculated as R= (G-1)/(N-1), where G is the number of distinct genotypes identified and N is the number of individuals (Dorken and Eckert 2001). Linkage disequilibrium (LD) was assessed using the association index $\overline{r_d}$ (Brown et al. 1980, modified by Agapow and Burt 2001) and computed using Multilocus v1.3b (Agapow and Burt 2001). Their significance was tested using 1000 permutations (Burt et al. 1996).

Single and multi-locus estimates of gene diversity were calculated as mean number of alleles per locus (N_a), expected heterozygosity (H_e, sensu Nei 1978) and observed heterozygosity (H_o) using Genetix 4.05 software (Belkhir et al. 1996-2004). Single- and multi-locus estimates of deviation from random mating (F_{IS}) were calculated according to Weir and Cockerham (1984) and significant was tested by running 1000 permutations using Genetix.

Genetix was also used to calculate the genetic differentiation (F_{ST}) between sites, and to compute the Mantel test, which evaluates the existence of a correlation between genetic and geographic distances. The possibility that *G. caudata* populations underwent a recent bottleneck event was evaluated using Bottleneck software v1.2.02 (Piry et al. 1999). Moreover, an AMOVA was implemented to test for the partition of genetic variance within sites, among sites within haplogroups and among haplogroups (haplogroups as defined with mitochondrial sequence dataset; Excoffier et al. 1992).

The Bayesian clustering method as implemented in Structure v2.3.4 software (Pritchard et al. 2000) was used to determine the existence of genetic groups within *G. caudata* populations categorising them into K sub-populations. A range of clusters (K), from one to eight was tested. Each

295 run, replicated 10 times, consisted of 400,000 iterations after a 'burn-in' of 200,000 iterations. K was
296 determined by the method developed by Evanno et al. (2005). Structure results were combined using
297 the greedy algorithm with 100,000 random input orders in Clummp (Jakobsson and Rosenberg 2007)
298 and visualised with the Distruct programme (Rosenberg 2004). The discriminant analysis of principal
299 components (DAPC, Jombart et al. 2010) calculated with the R software (R Development Core Team
300 2011) was used to investigate the relatedness across sites.
301
302 RESULTS
303
304 *Mitochondrial and chloroplast diversity*
305
306 Between 18 and 26 tetrasporophytes were sequenced per site for both the COI and *cox*2-3
307 markers producing 301 mitochondrial sequences in total (Table 1). After editing, an alignment of 630
308 base pairs (bp) was built from 157 individuals for COI. Twenty-one mitotypes and 21 polymorphic
309 sites were observed (GenBank accession numbers MF995393-MF995549). A total of 144 sequences
310 of *cox*2-3 (358 bp) revealed five polymorphic sites and six mitotypes (GenBank accession numbers
311 MG452409-MG452552). Once concatenated, the COI+*cox*2-3 sequences gave 26 mitotypes over the
312 983 bp studied on 144 individuals. After editing, an alignment of 1162 bp was built from 24
313 individuals for *rbc*L (i.e. 20 *G. caudata* and 4 *G. secunda*) and four chlorotypes and four
314 polymorphic sites were observed in *G. caudata*.
315 Maximum likelihood (ML) tree reconstruction for the concatenated COI+*cox*2-3 sequence
316 revealed the presence of two supported haplogroups distributed in distinct regions (Figure 2b). The
317 first group corresponded to a north-eastern lineage and included all individuals sampled in CE, RN,
318 PB and PE (i.e., ranging from 03°24'36"S to 08°07'59"S). The second group corresponded to a
319 south-eastern lineage and included all individuals sampled in ES and SP (i.e., ranging from

20°48'31"S to 23°55'01"S). The sequences of individuals sampled in BA were retrieved as a polytomy from which south-eastern (SE) and north-eastern (NE) clades emerged (Figure 2b). In the ML tree reconstructed for *rbc*L, *G. secunda* from Mexico and USA appeared as a sister species to *G. caudata* (Figure 2a). Within *G. caudata*, the ML tree was very poorly resolved. However, *G. caudata* from ES, SP and Santa Catarina State (SC, Brazil) formed a monophyletic, albeit non-supported, branch separated from all the other samples collected from the north-eastern coast of Brazil, the USA and Venezuela. For the *rbc*L, a single base pair difference was observed between samples collected in the north-east and south-east regions (0.09% of divergence between MF995550 and MF995560).

The haplotype network for the concatenated COI+*cox*2-3 sequences supports the phylogenetic results (Figure 3) and shows two main haplogroups. Seventeen haplotypes (i.e., C1-C17 in Figure 3) were found in the north-eastern part of the country in CE, RN, PB and PE. The two most widespread haplotypes, C1 and C5, were distributed in all four sites and the C13 haplotype was observed in the two adjacent sites of PB and PE. On the other hand, nine haplotypes (i.e., C18-C26 in Figure 3) were found in BA and in the south-eastern part of the country (ES and SP). No haplotypes were shared between the north-eastern and the BA plus south-eastern coasts or between sites sampled within the south-eastern haplogroup (Figure 3). Haplotype C25 was restricted to ES, C26 was restricted to SP, and seven haplotypes were private to BA. Concatenated mitotypes differed by 1-10 bp and only 2 bp separated the north-eastern and BA haplogroups (i.e., difference between C9 and C18 or C23, Figure 3).

A reduction in both gene (H) and nucleotide diversity (π) was observed from the north-eastern (NE) haplogroup to the BA and south-eastern monophyletic group (SE) for both mitochondrial markers ($p < 0.05$ for COI and *cox*2-3, Table 1). The AMOVA indicated that total genetic variance was mainly explained by the variance among haplogroups (COI 58.72%, *cox*2-3 71.22%; Table 2b). The variance within sites (COI 20.90%, *cox*2-3 16.18%) and the variance among sites within haplogroups (COI 20.38%, *cox*2-3 12.60%), although significant, were much lower (Table 2b). F_{ST}

values were significant between most pairs of sites, except for CE-RN ($p > 0.654$) and PB-PE ($p > 0.384$) for both markers, and for BA-ES ($p > 0.261$) for the *cox*2-3 (Table 2a). The Mantel tests showed a clear correlation between genetic and geographic distances for COI and for *cox*2-3 ($p < 0.005$) (Figure S1).

Microsatellite data: summary statistics, population differentiation and clustering analysis

A total of 411 diploid individuals (tetrasporophytes) of *G. caudata* were genotyped in this study and samples genotyped per site varied from 49 to 79 (Table 3). Fifteen polymorphic microsatellite markers were selected for the analyses, among the 17 loci previously developed to assess the genetic diversity of *G. caudata* (Ayres-Ostrock et al., 2016). The loci GraC_09 and GraC_11 were excluded due to very low amplification percentages (<57% and <47%, respectively).

The frequency of null alleles was significant for five loci (GraC_03, GraC_04, GraC_05, GraC_06 and GraC_12) and ranged from 0.070 to 0.349. Except for the RN site, which showed no evidence of null alleles for any locus, loci for which null alleles were detected and the frequency of null alleles varied with the site. The site with null alleles detected in the highest number of loci was SP (three loci) (Table 4). The number of alleles found in each site varied from one in CE, RN, PB, PE and SP for the locus GraC_10 to 16 for GraC_04 in the site of RN. Five loci were moderately polymorphic (4-6 alleles) and seven were highly variable (10-26 alleles) (Table 4). Evidence of linkage disequilibrium (LD) was found only in three of the seven sampled sites of *G. caudata*: CE, BA and SP. The locus GraC_03 showed strong and significant linkage disequilibrium with loci GraC_05 (SP, $\overline{r_d} = 0.492$ and $p < 0.036$) and GraC_07 (SP, $\overline{r_d} = 0.639$ and $p < 0.036$), as did the locus GraC_08 with locus GraBC_04 (CE, $\overline{r_d} = 0.262$ and $p < 0.011$). All 15 microsatellite loci were used in the following analyses.

Regardless of the site under study, all individuals analysed had unique multi-locus genotypes and values of clonal richness (R) were equal to one. Observed heterozygosity (H_o) ranged from 0.288 (SP) to 0.479 (RN) and expected heterozygosity (H_e) ranged from 0.284 (SP) to 0.458 (RN) (Table 3). The average number of alleles per locus varied among sites, with the highest value encountered in RN (5.267) and the lowest value in SP (3.400) (Table 3). The geographic pattern of genetic variation observed with the microsatellite markers resembled that observed with the mitochondrial sequences. Diversity was higher in the north-eastern area than in the south-eastern area (i.e., corresponding to north-eastern and BA+south-eastern mitochondrial haplogroups, respectively) and allelic richness (A_R) varied from 4.163 (NE) to 3.440 (BA+SE) and H_e varied from 0.446 (NE) to 0.363 (BA+SE). These differences were not significant ($p > 0.05$) (Table 3).

Estimates of the inbreeding coefficient (F_{IS}) varied among loci from 0.000 in loci GC_08 (ES and SP), GBC_01 (SP), GBC_03 (CE, PE and BA) and GBC_04 (BA) to one in the locus GC_12 (SP) (Table 4). Multi-locus F_{IS} values were generally close to zero and non-significant, except for ES (F_{IS} =-0.125) and BA (F_{IS} =0.115) (Table 3). The existence of a recent bottleneck in *G. caudata* was evaluated using Bottleneck software. Results indicate that all our sampled sites were in mutation-drift equilibrium. Unlike estimates previously obtained for mitochondrial markers, AMOVA analysis calculated using the microsatellites indicated that total genetic variance was mainly explained by the variance within sites 55.58% ($p < 0.0001$, Table 5b). The variance among haplogroups (29.34%, $p < 0.05$) and the variance among sites within haplogroups (15.07%, $p < 0.0001$), although significant, were lower (Table 5b). Moreover, estimates of genetic differentiation (F_{ST}) among sites of *G. caudata* ranged from 0.038 (PB-PE) up to 0.476 (SP-CE) (Table 5a). The Mantel test indicated that there was a clear correlation between genetic and geographic distances (Figure S2).

The Bayesian clustering method implemented in Structure software clearly showed that K =2 was the optimal number of clusters in our study (Figure 3c). For K =2, Structure results showed that all individuals from the north-eastern part of the coast (CE, RN, PB and PE) clustered together and

394 the three remaining sites of BA, ES and SP formed the other group. Except in BA, a very low level
395 of admixture was visible between the two genetic groups. When the Structure analysis was carried
396 out within each genetic group, K =3 clusters were encountered in the north-eastern and the
397 BA+south-eastern genetic group. Clustering within each geographic group generally separated the
398 distinct sites. The level of admixture was much higher in the north-eastern (NE) than in the BA+SE
399 (south-eastern) genetic group, where all individuals from the same site belonged to the same genetic
400 cluster. In the north-eastern genetic group, a high genetic similarity was observed between the two
401 neighbouring sites of PB and PE, with the individuals from PE showing traces of admixture between
402 two genetic groups (Figure 3c). A similar pattern of genetic structure was also observed in the
403 discriminant analysis of principal components (DAPC), where six clusters of genetically related
404 individuals were identified, mostly related to their sampling sites, except for PB and PE (Figure S3).
405 Allele size variation depended on the sampling region for three loci (GraC_03, GraBC_02 and
406 GraBC_03) (Figure 4). For GraC_03, private alleles were encountered in BA and in each of the two
407 most south-eastern sites (ES and SP) and only a low number of these (N=4) were observed in the
408 north-eastern part of *G. caudata* distribution at a very low frequency (Figure 4). For GraBC_02, one
409 frequent allele was observed in the three most south-eastern sites (i.e., BA, ES and SP; most common
410 allele size =258 bp), but another allele, present in high frequency, characterised the four most north-
411 eastern sites of CE, RN, PB and PE (most common allele size =264 bp) (Figure 4). For GraBC_02,
412 alleles 258 bp and 264 bp were not shared between the two genetic groups (i.e., between the north-
413 eastern and BA+south-eastern genetic group). For GraBC_03, the five north-eastern sites of CE, RN,
414 PB, PE and BA shared the same common allele, whereas another allele was encountered in samples
415 collected in the States of Espírito Santo (ES) and SP. In general, the sites of ES and SP from the
416 south-east presented a higher frequency of private alleles (0.177) than the north-east states (0.073)
417 and BA (0.068) (Table 3).
418

419 DISCUSSION

420

421 Throughout the Brazilian coast, two major genetic clusters, distributed in strict parapatry,
422 were revealed within the red alga *G. caudata* based on both phylogenetic inferences and population
423 genetic studies. There was a remarkable congruence between nuclear, mitochondrial and chloroplast
424 data showing a clear separation between the north-east (i.e., ranging from 03°S to 08°S) and the
425 south-east of the country (i.e., ranging from 20°S to 23°S), supporting the existence of a long-term
426 divergence along the Brazilian coast. The BA region (around 12°S) occupies an intermediate position
427 between both clades. These lineages also differ by their demographic histories: signatures of recent
428 demographic expansions in the north-east cluster, whereas the BA and south-eastern haplogroups are
429 composed of highly divergent populations, suggesting the maintenance of several different refugia.
430 Values of divergence observed between these haplogroups (*rbc*L 0.09% and COI 0.72%) are two
431 times lower than those obtained between the two northern and southern phylogeographic groups of
432 the intertidal *Hypnea pseudomusciformis* studied in the same geographic region (*rbc*L 0.2% and COI
433 1.3%) (Nauer et al. 2015, 2019). Nevertheless, these values are quite low when compared with pairs
434 of recently diverged red macroalgae species (*Iridaea cordata* cryptic species found on both side of
435 the Drake Passage, at the tip of South America in Tierra del Fuego and along the Antarctic
436 Peninsula: *rbc*L=3.17% and COI=8.31%, Ocaranza-Barrera et al. 2018; *Bostrychia intricata* cryptic
437 species N3 and N4 found in New Zealand Sub-Antarctic islands and New Zealand main islands:
438 *rbc*L=0.30% and COI=3.95%, Muangmai et al. 2015), driven and linked to historical events and
439 changing environments.

440 Estimates of divergence time in *G. caudata*, based on the percentage of divergence per
441 million years obtained in *I. cordata* and *B. intricata*, suggest that the effective separation between the
442 north-eastern (NE) and BA+south-eastern (SE) haplogroups occurred recently, during the
443 Quaternary, between 100,000 and 1,500,000 years ago. Apart from this major phylogenetic break

444 (between the PE and BA regions), mtDNA and microsatellite markers showed an additional level of
445 genetic structure, with each site located south of BA (i.e., ES, 20°S and SP, 23ºS) composed of a
446 single unique mtDNA haplotype and constituting strongly divergent nuclear group.
447
448 *A phylogeographic pattern dually influenced by marine and terrestrial climatic fluctuations in the*
449 *past*
450
451 The effect of the Pleistocene glacial cycles on the phylogeography of tropical species is much
452 less studied than that of temperate ones (Hewitt 2004). The effects of climatic change during the
453 Pleistocene in tropical and sub-tropical regions in southern America restricted species' distribution,
454 but allowed the persistence of populations (refugia), which remained isolated through multiple
455 glacial-interglacial oscillations (Lira et al. 2003). Therefore, strong signals of population expansion
456 during interglacial periods are generally not detected (Lessa et al. 2003). In the terrestrial realm,
457 studies suggest that there were three Late Quaternary (with the most recent glacial period occurring
458 between about 120,000 and 20,000 years before present) main refugia in the rainforest located along
459 the Brazilian Atlantic coast (i.e. in the regions of PE, BA and SP), which fostered the long-term
460 persistence of genetically isolated lineages (Carnaval and Moritz 2008, Carnaval et al. 2009).
461 Interestingly, these three main terrestrial refugia (see Figure 1) fit well with the two main
462 phylogeographic breaks revealed in this study and correspond to areas where a high level of private
463 alleles and haplotypes were detected in *G. caudata*.
464 The phylogeographic structure of marine species has been shaped by sea-level fluctuations
465 during the Pleistocene (Suguio et al. 1985, Martin et al. 2003) as well as ocean current circulation
466 patterns. Similar to our study, several phylogeographic studies have described one or two major
467 genetic breaks along the Brazilian coast in invertebrate and vertebrate marine species (in the king
468 weakfish, *Macrodon ancylodon,* Santos et al. 2006; in the silver fish *Atherinella brasiliensis*, da

Silva Cortinhas et al. 2016; in the king fish *Menticirrhus americanus*, dos Santos Freitas et al. 2017; in the white shrimp *Litopenaeus schmitt* Maggioni et al. 2003; in the coral *Mussismilia hispida* Peluso et al. 2018) and in the red mangrove tree *Rhizophora mangle* (Francisco et al. 2018). However, the exact limits of the breaks do not always coincide among the studied species. In most studies, the first genetic barrier is located at 4°S-6°S, separating the populations of northern Brazil from those of central Brazil (Santos et al. 2006, Francisco et al. 2018, Peluso et al. 2018) and the second one occurs at 21°S-23°S, separating the tropical populations located along the coast where the Brazil Current flows from the sub-tropical populations influenced by cooler South Atlantic Central Waters (SACW) (Santos et al. 2006, da Silva Cortinhas et al. 2016, dos Santos Freitas et al. 2017, Peluso et al. 2018). All these studies suggest ocean currents (Figure 1) play a role as effective barriers to gene flow.

In intertidal organisms, such as *G. caudata*, the phylogeographic structure is probably best explained by the interaction between terrestrial history and marine current patterns. Other features such as the outflows from the Doce and São Francisco rivers may also act as biogeographical barriers separating populations located along the Brazilian coast (Schmid et al. 1995, Carnaval et al. 2009, Figure 1). Indeed, even if *G. caudata* has been described as euryhaline species (Yokoya and Oliveira 1992), experiments have shown that it was not able to grow at salinities lower than 15 PSU (de Miranda et al. 2012) and it can be assumed that strong freshwater outflows may have a significant impact on the fitness of these intertidal populations. The possible role of the São Francisco River as a promoter of differentiation has been commonly reported in terrestrial organisms (Pellegrino et al. 2005, Carnaval and Moritz 2008, Carnaval et al. 2009). However, there is congruence between river systems and the borders of putative long-term refugia in the area (Carnaval and Moritz 2008), and some authors have proposed that primary divergence was due to isolation in climatic refugia, rivers being only secondary barriers maintaining the resulting genetic structure (Carnaval et al. 2014; but see Thomé et al. 2014). Additionally, along the Brazilian coast, the Holocene sea-level history

494 suggests regional variations, with alternating periods of mean sea-level rise and fall resulting in huge
495 reductions in population size and decreased connectivity. The frequency, time and impact of these
496 oscillations during the past 7000 years have been well studied (Angulo and Lessa 1997, Martin et al.
497 1998, Lessa and Angulo 1998, Martin et al. 2003) and these oscillations have had a strong influence
498 on the distribution and diversity of several coastal species (e.g., in the sand dune ant *Mycetophylax*,
499 Cardoso et al. 2015; in five small mammal species widespread in the Brazilian Atlantic forest, Leite
500 et al. 2016; and in the red mangrove *Rhizophora mangle*, Pil et al. 2011). Depending on the study,
501 sea-level fluctuations had amplitudes of 2 to 4 m when compared to today's sea-level, and durations
502 of 400 to 500 years (Suguio et al. 1985, Martin et al. 2003). These oscillations were characterized by
503 rates in sea level change of 16 up to 32 mm per year, three times faster than the fastest sea-level rise
504 period (10 mm/year, between 15000 and 8000 yr BP - Angulo et al. 2006), that could have strongly
505 affected marine species distribution along the RN-SC coast and in adjacent regions (Fleming et al.
506 1998). Strikingly, receding sea levels exposed as much as 92% of today's Brazilian continental shelf
507 (Araújo et al. 2008, Carnaval et al. 2009), with significantly more land being exposed south of BA
508 (i.e., Abrolhos Bank,18^{o}S) (Leite et al. 2016). There are many reports worldwide of genetic evidence
509 of bottlenecks in coastal marine taxa in tropical regions due to the global reduction in sea level
510 during the Pleistocene (Ludt and Rocha 2015). Such climatic events may explain the reduced
511 mitochondrial and nuclear genetic diversity and high genetic structure observed between sites of *G.*
512 *caudata* located south of BA (ES and SP) compared with the north-eastern sites. Moreover, the
513 fluctuation of the sea levels along the Vitoria-Trindade Ridge was reported as a possible cause of the
514 high level of endemism in this coral reef environment because of successive bottlenecks (Pinheiro et
515 al. 2017). Our hypothesis is that such successive bottlenecks will impact more strongly the genetic
516 structure of intertidal benthic organisms rather than subtidal pelagic species.
517
518 *Secondary contact zone, but low level of admixture in the Bahia (BA) region*

519

520 The Bahia (BA) region presents a high number of divergent haplotypes, suggesting that one
521 large or several refugia may have withstood the successive glacial cycles of the Pleistocene in this
522 region. Mitochondrial markers point out the existence of large and stable populations in BA,
523 historically isolated from both the south-eastern and the north-eastern parts of the *G. caudata*
524 distribution in Brazil. The existence of major long-standing BA refugia in the coastal Brazil Atlantic
525 forest has also been demonstrated for terrestrial plants and animals and is associated with higher
526 species and genetic endemism, compared with areas located south of the Doce River (i.e., our sites of
527 ES and SP) (Carnaval and Moritz 2008, Carnaval et al. 2009). In *G. caudata*, the mtDNA tree shows
528 that individuals sampled in this region constitute a basal polytomy to both the north-eastern and
529 south-eastern monophyletic branches. This result is supported by the private BA haplotypes, which
530 occupy an intermediate position in the mtDNA haplotype network, connecting the northern-most and
531 southern-most haplotypes. However, depending on the locus, diagnostic microsatellite alleles of the
532 north-eastern and south-eastern regions were both observed in the BA population (Figure 4) and BA
533 was the only case in which a low level of admixture between the north-eastern and south-eastern
534 lineages was detected. All these results suggest that BA may correspond not only to a refugium, but
535 also to a recent secondary contact zone between the highly differentiated north-eastern and south-
536 eastern regions. The occurrence of a contact zone in the BA region can also be surmised from a
537 previous phylogenetic study conducted in another red alga species (*H. pseudomusciformis,* Nauer et
538 al. 2019). As in *G. caudata*, a clear divergence between the samples from north-east and the samples
539 from the south-east of Brazil was detected using COI mitochondrial sequences and, in both studies,
540 the BA region is an intermediate region that is either grouped with the north-eastern (in *H.*
541 *pseudomusciformis*) or with the south-eastern cluster (in *G. caudata*).

542 Both historical isolation and more recent micro-evolutionary processes have probably played a
543 major role in shaping *G. caudata* genetic structure in the BA region. Although we did not observe the

544 gradient of admixture and/or clines of allele frequencies expected in this contact zone, more
545 extensive sampling in this zone is required to clarify the size of the contact zone and level of
546 introgression between the two main lineages. It is possible that the genetic structure is currently
547 maintained by the combination of the low dispersal capacity of the species, the existence of various
548 barriers to gene flow and adaptation to sharp changes in environmental conditions (e.g., salinity, sea
549 surface temperature, oxygen and nutrient concentration; Briani et al. 2018). In seaweeds with low
550 dispersal capacity, even weak and/or transient barriers can easily promote and maintain strong
551 genetic divergence (Montecinos et al. 2012). Studies on different intertidal red seaweed species
552 revealed restricted gene flow even at short distance. Particularly between tide pools located at
553 different levels of the shore and exposed to contrasting levels of physiological stress (Engel et al.
554 1999, 2004, Krueger-Hadfield et al. 2011, 2013, 2015, Maggs et al 2011). Such patterns of reduced
555 gene flow, if congruent with contrasted environmental conditions, may also initiate ecotypic
556 differentiation. Briani et al. (2018) reported that the content of mycosporine-like amino acids
557 (MAAs) in 39 different red algae including *G. caudata* varies sharply between the north-east and
558 south-east of the Brazilian coast. Algae MAAs content varied mainly according to the level of UV
559 and irradiance, however, other environmental factors such as pH and phosphate and nitrate
560 concentrations in the water column also had some influence (Briani et al. 2018). The genetic break
561 revealed in *G. caudata* thus fits nicely with the sharp abiotic environmental break detected between
562 tropical and subtropical regions (Briani et al. 2018).
563
564 *Ecotypic differentiation and conservation management issues*
565
566 Differences in physiological performance (e.g., growth rate, photosynthesis parameters,
567 pigment content and sensitivity to UVB radiation) were observed between strains of *G. caudata* from
568 CE (corresponding to the NE clade) and SP (corresponding to the SE group) grown in controlled

laboratory conditions (Araújo et al. 2014, Faria et al. 2017). Possible ecotypic differentiation may have arisen along the *G. caudata* distribution range, linked to local adaptation to habitats specific to the north-east and the regions of lower latitude (such as MAAs content, see Briani et al. 2018). These results were also confirmed by the Mantel test that showed a significant correlation between genetic and geographic distances, suggesting that the population structure and the subsequent occurrence of ecotypic differentiation could be explained by an isolation-by-distance model.

Interestingly, differences in seawater temperature linked to ocean circulation patterns have also been detected along the Brazilian coast (average ranging between 20 and 28°C in the northeast region and between 6 and 24°C in the southeast region); and are regarded as a potential physiological barrier to gene flow for some species of fish (Galetti et al. 2006, Santos et al. 2006, Machado et al. 2017). Temperature ecotypes have been described along the Brazilian coast for another *Gracilaria* species: *G. birdiae* (Ursi et al. 2003). Differences in sensitivity to UVB radiation were also detected between *G. birdiae* strains from CE and SP states (Ayres and Plastino 2014). Physiological divergence between habitats, linked to distinct resilience capacity to temperature fluctuation and emersion (i.e., desiccation) stress, has been shown in other intertidal seaweeds, for example in the brown alga *Fucus vesiculosus* (Nicastro et al. 2013, Saada et al. 2016). Ecotypic divergence has been shown to lead to rapid speciation in several organisms including macroalgae (i.e., adaptation to low salinity in the Baltic sea in *Fucus* in the time span of a few hundreds of years, Pereyra et al. 2009). Nevertheless, a recent study, based on experimental crosses, demonstrated that individuals of *G. caudata* from north-eastern (i.e, CE) and south-eastern (i.e, ES and SP) clades produced viable and fertile descendants, suggesting that complete reproductive barriers may not yet have evolved between the two clades (Chiaramonte et al. 2018).

In conclusion, our study demonstrates the existence of divergent clades — which based on previous physiological work may correspond to distinct ecotypes (Araújo et al. 2014, Faria et al. 2017) — in *G. caudata* and thus should be considered for the management policy of this

commercially important species. Harvesting of natural *Gracilaria* beds in Brazil has gradually diminished since the 1970s and has been replaced by small-scale cultivation (Hayashi et al. 2014). Nevertheless, since the beginning of this activity in the 1960s, over-harvesting of the natural beds in the north-eastern region has compromised one of the main sources of genetic diversity. Acknowledging the existence of multiple phylogeographical lineages along the Brazilian coast is important not only for understanding the recent historical processes shaping genetic diversity in these tropical and sub-tropical regions, but also for developing effective conservation strategies, particularly in an environment subject to important anthropogenic factors like overharvesting, habitat fragmentation and degradation.

ACKNOWLEDGMENTS

This research was supported by the São Paulo Research Foundation (FAPESP: 2010/50175-3; 2011/10189-8), the Brazilian National Council for Scientific and Technological Development (CNPq: 300148/93-3; 301491/2013-5), the programme of international cooperation USP/COFECUB between the University of São Paulo and the *Comité Français d'Evaluation de la Coopération Universitaire avec le Brésil* and the International Research Network DEBMA 'Diversity, Evolution and Biotechnology of Marine Algae' (GDRI CNRS 0803). This study was funded in part by the *Coordenação de Aperfeiçoamento de Pessoal de Nível Superior - Brasil* (CAPES) - Finance Code 001. We are also most grateful to the Biogenouest Genomics core facility for its technical support. We thank the anonymous referees for valuable suggestions.

BIOSKETCH

Author contributions: L.A-O., E.M.P. and C.D. conceived the study. L.A-O. and E.M.P. conducted the field work. L.A-O. and S.M. generated the data and L.A-O., C.D., M-L.G., and M.V. performed the data analyses. L.A-O. wrote the first draft of the manuscript. All authors contributed to the last draft of the manuscript.

CONFLICT OF INTEREST STATEMENT

The authors declare no conflict of interest

REFERENCES

Agapow, P. M. & Burt, A. 2001. Indices of multilocus linkage disequilibrium. *Mol. Ecol. Notes*. 1:101–102.

Angulo, R. J. & Lessa, G. C. 1997. The Brazilian sea-level curves: a critical review with emphasis on the curves from the Paranaguá and Cananéia regions. *Mar. Geol.* 140:141-166.

Angulo, R. J., Lessa, G. C. & de Souza, M. C. 2006. A critical review of mid-to late-Holocene sea-level fluctuations on the eastern Brazilian coastline. *Quat. Sci. Rev.* 25:486-506.

Araújo, F. O., Ursi, S. & Plastino, E. M. 2014. Intraspecific variation in *Gracilaria caudata* (Gracilariales, Rhodophyta): growth, pigment content, and photosynthesis. *J. Appl. Phycol.* 26:849-858.

Araújo, M. B., Nogués-Bravo, D., Diniz-Filho, J. A. F., Haywood, A. M., Valdes, P. J. & Rahbek, C. 2008. Quaternary climate changes explain diversity among reptiles and amphibians. *Ecography.* 31:8-15.

642 Arnaud-Haond, S. & Belkhir, K. 2007. GENECLONE: a computer program to analyse genotypic
643 data, test for clonality and describe spatial clonal organization. *Mol. Ecol. Notes*. 7:15–17.
644 Assis, J., Coelho, N. C., Lamy, T., Valero, M., Alberto, F. & Serrão, E. Á. 2016. Deep reefs are
645 climatic refugia for genetic diversity of marine forests. *J. Biogeogr.* 43:833-844.
646 Avise, J. C. 2000. *Phylogeography. The history and formation of species*. Cambridge, Massachusetts
647 and London: Harvard University Press, 464 pp.
648 Ayres-Ostrock, L. M. & Plastino, E. M. 2014. Effects of UV-B radiation on growth rates, pigment
649 content and ultrastructure of red (wild type), greenish-brown and green strains of Gracilaria
650 birdiae (Gracilariales, Rhodophyta). *Eur. J. Phycol* 49:197-212.
651 Ayres-Ostrock, L. M. 2014. Estudos populacionais em *Gracilaria birdiae* e *G. caudata*
652 (Gracilariales, Rhodophyta): aspectos fenológicos, fisiológicos e moleculares. Ph.D.
653 dissertation. University of São Paulo, São Paulo, 203 pp.
654 Ayres-Ostrock, L. M., Mauger, S., Plastino, E. M., Oliveira, M. C., Valero, M. & Destombe, C.
655 2015. Development and characterization of microsatellite markers in two agarophyte
656 species, *Gracilaria birdiae* and *Gracilaria caudata* (Gracilariaceae, Rhodophyta), using
657 next-generation sequencing. *J. Appl. Phycol.* 28:653-662.
658 Bandelt, H. J., Forster, P. & Röhl. A. 1999. Median-joining networks for inferring intraspecific
659 phylogenies. *Mol. Biol. Evol.* 16:37-48.
660 Belkhir, K., Borsa, P., Chikhi, L., Raufaste, N. & Bonhomme, F. 1996–2004. GENETIX 4.05,
661 logiciel sous Windows TM pour la génétique des populations. Laboratoire Genome,
662 Populations, Interactions, CNRS UMR 5000, Universite´ de Montpellier II, Montpellier,
663 France. URL:http://www.genetix.univmontp2.fr/genetix/intro.htm
664 Bellorin, A. M., Oliveira, M. C. & Oliveira, E. C. 2004. *Gracilaria vermiculophylla*: a western
665 Pacific species of Gracilariaceae (Rhodophyta) first recorded from the eastern Pacific.
666 *Phycol. Res.* 52:69–79.

667 Benzie, J. A. H. 1998. Genetic structure of marine organisms and SE Asian biogeography. *Biogeogr.*
668 *Geol. Evol. SE Asia*. 30:197-209.
669 Briani, B., Sissini, M. N., Lucena, L. A., Batista, M. B., Costa, I. O., Nunes, J. M., Schmitz, C., …
670 Barufi, J. B. 2018 The influence of environmental features in the content of
671 mycosporine-like amino acids in red marine algae along the Brazilian coast. *Journal of*
672 *Phycology*. DOI: 10.1111/jpy.12640.
673 Bringloe, T. T. & Saunders, G. W. 2018. Mitochondrial DNA sequence data reveal the origins of
674 postglacial marine macroalgal flora in the Northwest Atlantic. *Mar. Ecol. Prog. Ser*. 589:45-
675 58.
676 Brown, A. H. D., Feldman, M. W. & Nevo, E. 1980. Multilocus structure of natural populations of
677 *Hordeum spontaneum. Genetics.* 96:523-536.
678 Brunelli, B. 2017. Filogeografia de *Gelidium floridanum* e *Pterocladiella capillacea* (Gelidiales,
679 Rhodophyta) e espécies relacionadas no Atlântico ocidental, com ênfase no Brasil, com base
680 em dados morfológicos e moleculares. Dissertação de Mestrado, Instituto de Botânica de
681 São Paulo, 84 pp.
682 Burt, A., Carter, D. A., Koenig, G. L., White, T. J. & Taylor, J. W. 1996. Molecular markers reveal
683 cryptic sex in the human pathogen *Coccidioides immitis*. *Proc. Natl. Acad. Sci. USA*.
684 93:770-773.
685 Cardoso, D. C., Cristiano, M. P., Tavares, M. G., Schubart, C. D. & Heinze, J. 2015. Phylogeography
686 of the sand dune ant *Mycetophylax* simplex along the Brazilian Atlantic Forest coast:
687 remarkably low mtDNA diversity and shallow population structure. *BMC Evol. Biol.*
688 15:106.
689 Carnaval, A. C. & Moritz, C. 2008. Historical climate modelling predicts patterns of current
690 biodiversity in the Brazilian Atlantic forest. *J. Biogeogr.* 35:1187-1201.

691 Carnaval, A. C., Hickerson, M. J., Haddad, C. F., Rodrigues, M. T. & Moritz, C. 2009. Stability
692 predicts genetic diversity in the Brazilian Atlantic forest hotspot. *Science*. 323:785-789.
693 Carnaval, A. C., Waltari, E., Rodrigues, M. T., Rosauer, D., VanDerWal, J., Damasceno, R., Prates,
694 v., ... Moritz, C. 2014. Prediction of phylogeographic endemism in an environmentally
695 complex biome. *Proc. R. Soc. Lond. B. Biol. Sci.* 281:20141461.
696 Chiaramonte, A. R., Parra, P. A., Ayres-Ostrock, L. M. & Plastino, E. M. 2018. *Gracilaria caudata*
697 (Gracilariales, Rhodophyta) is reproductively compatible along the whole Brazilian coast. *J.*
698 *Appl. Phycol.* https://doi.org/10.1007/s10811-018-1642-8
699 Cohen, S., Faugeron, S., Martínez, E. A., Correa, J. A., Viard, F., Destombe, C. & Valero, M. 2004.
700 Molecular identification of two sibling species under the name *Gracilaria chilensis*
701 (Rhodophyta, Gracilariales). *J. Phycol.* 40:742-747.
702 Costa, E. S., Plastino, E. M., Petti, R., Oliveira, E. C. & Oliveira, M. C. 2012. The Gracilariaceae
703 Germplasm Bank of the University of São Paulo, Brazil—a DNA barcoding approach. *J.*
704 *Appl. Phycol.* 24:1643-1653.
705 Costa, L. P., Leite, Y. L. & Patton, J. L. 2003. Phylogeography and systematic notes on two species
706 of gracile mouse opossums, genus *Gracilinanus* (Marsupialia: Didelphidae) from Brazil.
707 *Proc. Biol. Soc. Wash.* 116:275-292.
708 Couceiro L, Robuchon M, Destombe C, Valero M (2013) Management and conservation of the kelp
709 species *Laminaria digitata*: using genetic tools to explore the potential exporting role of the
710 MPA "Parc naturel marin d'Iroise". *Aquat. Living Resour*. 26:197-205.
711 da Silva Cortinhas, M. C., Kersanach, R., Proietti, M., Dumont, L. F. C., D'Incao, F., Lacerda, A. L.
712 F., Prata, P. S., … Cestari, M. M. 2016. Genetic structuring among silverside fish
713 (*Atherinella brasiliensis*) populations from different Brazilian regions. *Estuar. Coast. Shelf.*
714 *Sci.* 178:148-157.

715 Davis, M. B. & Shaw, R. G. 2001. Range shifts and adaptive responses to Quaternary climate
716 change. *Science*. 292:673-679.
717 de Miranda, G. E., Yokoya, N. S. & Fujii, M. T. 2012. Effects of temperature, salinity and irradiance
718 on carposporeling development of *Hidropuntia caudata* (Gracilariales, Rhodophyta). *Rev.*
719 *Bras. Farmacogn*. 22:818-824.
720 Destombe, C., Valero, M. & Guillemin, M. L. 2010. Delineation of two sibling red algal species,
721 *Gracilaria gracilis* and *Gracilaria dura* (Gracilariales, Rhodophyta), using multiple DNA
722 markers: resurrection of the species *G. dura* previously described in the Northern Atlantic
723 200 years ago. *J. Phycol.* 46:720-727.
724 Dorken, M. E. & Eckert, C. G. 2001. Severely reduced sexual reproduction in northern populations
725 of a clonal plant, *Decodon verticillatus* (Lythraceae). *J. Ecol.* 89:339–350.
726 dos Santos Freitas, A., da Silva, R., Sampaio, I. & Schneider, H. 2017. The mitochondrial control
727 region reveals genetic structure in southern kingcroaker populations on the coast of the
728 Southwestern Atlantic. *Fish. Res.* 191:87-94.
729 Engel, C. R., Destombe, C. & Valero, M. 2004. Mating system and gene flow in the red seaweed
730 *Gracilaria gracilis*: effect of haploid–diploid life history and intertidal rocky shore
731 landscape on fine-scale genetic structure. *Heredity*. 92:289.
732 Engel, C. R., Wattier, R., Destombe, C. & Valero, M. 1999. Performance of non–motile male
733 gametes in the sea: analysis of paternity and fertilization success in a natural population of a
734 red seaweed, *Gracilaria gracilis*. *Proc. R. Soc. Lond. B Biol. Sci.* 266:1879-1886.
735 Evanno, G., Regnaut, S. & Goudet, J. 2005. Detecting the number of clusters of individuals using the
736 software structure: a simulation study. *Mol. Ecol.* 14:2611–2620.
737 Excoffier, L. & Lischer, H. E. 2010. Arlequin suite ver 3.5: a new series of programs to perform
738 population genetics analyses under Linux and Windows. *Mol. Ecol. Resour.* 10:564-567.

739 Excoffier, L., Smouse, P. E. & Quattro, J. M. 1992. Analysis of molecular variance inferred from
740 metric distances among DNA haplotypes: application to human mitochondrial DNA
741 restriction data. *Genetics*. 131:479-491.
742 Faria, A. V. & Plastino, E. M. 2016. Physiological assessment of the mariculture potential of a
743 *Gracilaria caudata* (Gracilariales, Rhodophyta) variant. *J. Appl. Phycol.* 28:2445-2452.
744 Faria, A. V., Bonomi-Barufi, J. & Plastino, E. M. 2017. Ecotypes of *Gracilaria caudata*
745 (Gracilariales, Rhodophyta): physiological and morphological approaches considering life
746 history phases. *J. Appl. Phycol.* 29:707-719.
747 Francisco, P. M., Mori, G. M., Alves, F. M., Tambarussi, E. V. & de Souza, A. P. 2018. Population
748 genetic structure, introgression, and hybridization in the genus Rhizophora along the
749 Brazilian coast. *Ecol. Evol.* 8:3491-3504.
750 Freshwater, D. W., Fredericq, S., Butler, B. S., Hommersand, M. H. & Chase, M. W. 1994. A gene
751 phylogeny of the red algae (Rhodophyta) based on plastid *rbc*L. *Proc. Natl. Acad. Sci.*
752 91:7281-7285.
753 Fu, Y. X. 1997. Statistical tests of neutrality of mutations against population growth, hitchhiking and
754 background selection. *Genetics*. 147:915-925.
755 Galetti Jr, P. M., Molina, W. F., Affonso, P. R. A. & Aguilar, C. T. 2006. Assessing genetic diversity
756 of Brazilian reef fishes by chromosomal and DNA markers. *Genetica*. 126:161-177.
757 Gomes da Silva, P., Dalinghaus, C., González, M., Gutiérrez, O., Espejo, A., Abascal, A. J. & Klein,
758 A. H. 2016. Estimating flooding level through the Brazilian coast using reanalysis data. *J.*
759 *Coast. Res.* 75:1092-1096.
760 Guillemin, M. L., Dubrasquet, H., Reyes, J. & Valero, M. 2018. Comparative phylogeography of six
761 red algae along the Antarctic Peninsula: extreme genetic depletion linked to historical
762 bottlenecks and recent expansion. *Polar Biol.* 41:827-837.

763 Guillemin, M. L., Faugeron, S., Destombe, C., Viard, F., Correa, J. A. & Valero, M. 2008. Genetic
764 variation in wild and cultivated populations of the haploid–diploid red alga *Gracilaria*
765 *chilensis*: how farming practices favor asexual reproduction and heterozygosity. *Evolution*.
766 62:1500-1519.
767 Guillemin, M. L., Valero, M., Faugeron, S., Nelson, W. & Destombe, C. 2014. Tracing the trans-
768 Pacific evolutionary history of a domesticated seaweed (*Gracilaria chilensis*) with
769 archaeological and genetic data. *PloS one*. 9: e114039.
770 Guillemin, M. L., Valero, M., Tellier, F., Macaya, E. C., Destombe, C. & Faugeron, S. 2016.
771 Phylogeography of seaweeds in the South East Pacific: complex evolutionary processes
772 along a latitudinal gradient. *In* Zi-Min, H. & Ceridwen, F. [Eds.] *Seaweed Phylogeography*.
773 Springer, Dordrecht, pp. 251-277.
774 Gurgel, C. F. D., Norris, J. N., Schmidt, W. E., Le, H. N. & Fredericq, S. 2018. Systematics of the
775 Gracilariales (Rhodophyta) including new subfamilies, tribes, subgenera, and two new
776 genera, *Agarophyton* gen. nov. and *Crassa* gen. nov. *Phytotaxa.* 374:1-23.
777 Hall, T. A. 1999, January. BioEdit: a user-friendly biological sequence alignment editor and analysis
778 program for Windows 95/98/NT. *Nucleic Acids Symp. Ser.* 41:95-98.
779 Hampe, A. & Petit, R. J. 2005. Conserving biodiversity under climate change: the rear edge matters.
780 *Ecol. Lett.* 8:461-467.
781 Haq, B. U., Hardenbol, J. & Vail, P. R. 1987. Chronology of fluctuating sea levels since the Triassic.
782 *Science.* 235:1156-1167.
783 Hasegawa, M., Kishino, H. & Yano, T. A. 1985. Dating of the human-ape splitting by a molecular
784 clock of mitochondrial DNA. *J. Mol. Evol.* 22:160-174.
785 Hayashi, L., Bulboa, C., Kradolfer, P., Soriano, G. & Robledo, D. 2014. Cultivation of red seaweeds:
786 a Latin American perspective. *J. Appl. Phycol.* 26:719-727.

787 Hewitt, G. M. 1996. Some genetic consequences of ice ages, and their role in divergence and
788 speciation. *Biol. J. Linnean. Soc*. 58:247-276.
789 Hewitt, G. M. 2000. The genetic legacy of the Quaternary ice ages. *Nature*. 405: 907-913.
790 Hewitt, G. M. 2004. Genetic consequences of climatic oscillations in the Quaternary. *Philos. Trans.*
791 *R. Soc. Lond. B. Biol. Sci.* 359:183-195.
792 Hu, Z. M., Duan, D. L. & Lopez-Bautista, J. 2016. Seaweed phylogeography from 1994 to 2014: an
793 overview. *In* Zi-Min, H. & Ceridwen, F. [Eds.] *Seaweed Phylogeography*. Springer,
794 Dordrecht, pp. 3-22.
795 Iha, C., Grassa, C. J., Lyra, G. M., Davis, C.C., Verbruggen, H. & Oliveira, M. C. 2018. Organellar
796 genomics: a useful tool to study evolutionary relationships and molecular evolution in
797 Gracilariaceae (Rhodophyta). *J. Phycol*. 54:775-787.
798 Jakobsson, M. & Rosenberg, N. A. 2007. CLUMPP: a cluster matching and permutation program for
799 dealing with label switching and multimodality in analysis of population structure.
800 *Bioinformatics*. 23:1801-1806.
801 Jolliffe, I. T. 2002. Graphical representation of data using principal components. *In* Jolliffe, I. T.
802 [Eds.] *Principal component analysis*. Springer Series in Statistics, Springer, New York, NY,
803 pp. 78-110.
804 Jombart, T., Devillard, S. & Balloux, F. 2010. Discriminant analysis of principal components: a new
805 method for the analysis of genetically structured populations. *BMC Genet.* 11:94.
806 Kalyaanamoorthy, S., Minh, B. Q., Wong, T. K., von Haeseler, A. & Jermiin, L. S. 2017.
807 ModelFinder: fast model selection for accurate phylogenetic estimates. *Nat. Methods.*
808 14:587-589.
809 Krueger-Hadfield, S. A., Collen, J., Daguin-Thiébaut, C. & Valero, M. 2011. Genetic population
810 structure and mating system in Chondrus crispus (Rhodophyta). J. Phycol. 47:440-450.

Krueger-Hadfield, S. A., Kollars, N. M., Byers, J. E., Greig, T. W., Hammann, M., Murray, D. C., Murren, C. J. & Sotka, E. E. 2016. Invasion of novel habitats uncouples haplo-diplontic life cycles. *Mol. Ecol.* 25:3801-3816.

Krueger-Hadfield, S. A., Roze, D., Correa, J. A., Destombe, C., & Valero, M. 2015. O father where art thou? Paternity analyses in a natural population of the haploid–diploid seaweed *Chondrus crispus*. *Heredity*. 114:185.

Krueger-Hadfield, S. A., Roze, D., Mauger, S. & Valero, M. 2013. Intergametophytic selfing and microgeographic genetic structure shape populations of the intertidal red seaweed *Chondrus crispus*. Mol. Ecol. 22:3242-3260.

Leite, Y. L., Costa, L. P., Loss, A. C., Rocha, R. G., Batalha-Filho, H., Bastos, A. C., Quaresma, V. S. & Pardini, R. 2016. Neotropical forest expansion during the last glacial period challenges refuge hypothesis. *Proc. Natl. Acad. Sci.* 113:1008-1013.

Lessa, E. P., Cook, J. A. & Patton, J. L. 2003. Genetic footprints of demographic expansion in North America, but not Amazonia, during the Late Quaternary. *Proc. Natl. Acad. Sci.* 100:10331-10334.

Lessa, G. C. & Angulo, R. J. 1998. Oscillations or not oscillations, that is the question-reply. M*ar. Geol.* 150:189-196.

Lira, C. F., Cardoso, S. R. S., Ferreira, P. C. G., Cardoso, M. A. & Provan, J. 2003. Long-term population isolation in the endangered tropical tree species *Caesalpinia echinata* Lam. revealed by chloroplast microsatellites. *Mol. Ecol.* 12:3219-3225.

Ludt, W. B. & Rocha, L. A. 2015. Shifting seas: the impacts of Pleistocene sea-level fluctuations on the evolution of tropical marine taxa. *J. Biogeogr.* 42:25-38.

Lyra, G. D. M., Gurgel, C. F. D., Costa, E. D. S., de Jesus, P. B., Oliveira, M. C., Oliveira, E. C., Davis, C. C. & Nunes, J. M. D. C. 2016. Delimitating cryptic species in the *Gracilaria*

domingensis complex (Gracilariaceae, Rhodophyta) using molecular and morphological data. *J. Phycol.* 52:997-1017.

Machado, L. F., de Souza Damasceno, J., Bertoncini, Á. A., Farro, A. P. C., Hostim-Silva, M. & Oliveira, C. 2017. Population genetic structure and demographic history of the spadefish, *Chaetodipterus faber* (Ephippidae) from Southwestern Atlantic. *J. Exp. Mar. Biol. Ecol.* 487:45-52.

Maggioni, R., Rogers, A. D. & Maclean, N. 2003. Population structure of *Litopenaeus schmitti* (Decapoda: Penaeidae) from the Brazilian coast identified using six polymorphic microsatellite loci. *Mol. Ecol.* 12:3213-3217.

Maggs, C. A., Castilho, R., Foltz, D., Henzler, C., Jolly, M. T., Kelly, J., Olsen, J., … Wares, J. 2008. Evaluating signatures of glacial refugia for North Atlantic benthic marine taxa. *Ecology.* 89:S108-S122.

Maggs, C. A., Fletcher, H. L., Fewer, D., Loade, L., Mineur, F. & Johnson, M. P. 2011. Speciation in red algae: members of the Ceramiales as model organisms. *Integr. Comp. Biol.* 51:492-504.

Martin, L., Bittencourt, A. C. S. P., Flexorc, J. M. & Suguiod, K. 1998. Oscillations or not oscillations, that is the question: Comment on Angulo, RJ and Lessa, GC "The Brazilian sea-level curves: a critical review with emphasis on the curves from the Paranaguá and Cananéia regions" [Mar. Geol. 140, 141–166]. *Mar. Geol.* 150:179-187.

Martin, L., Dominguez, J. M. & Bittencourt, A. C. 2003. Fluctuating Holocene sea levels in eastern and southeastern Brazil: evidence from multiple fossil and geometric indicators. *J. Coastal Res.* 101-124.

Minh, B. Q., Nguyen, M. A. T. & von Haeseler, A. 2013. Ultrafast approximation for phylogenetic bootstrap. *Mol. Biol. Evol.* 30:1188-1195.

858 Montecinos, A., Broitman, B. R., Faugeron, S., Haye, P. A., Tellier, F. & Guillemin, M. L. 2012.
859 Species replacement along a linear coastal habitat: phylogeography and speciation in the red
860 alga *Mazzaella laminarioides* along the south east pacific. *BMC Evol. Biol.* 12:97.
861 Muangmai, N., Fraser, C. I. & Zuccarello, G. C. 2015. Contrasting patterns of population structure
862 and demographic history in cryptic species of *Bostrychia intricata* (Rhodomelaceae,
863 Rhodophyta) from New Zealand. *J. Phycol.* 51:574-585.
864 Nauer, F., Cassano, V. & Oliveira, M. C. 2015. Description of *Hypnea pseudomusciformis sp. nov.*, a
865 new species based on molecular and morphological analyses, in the context of the *H.*
866 *musciformis* complex (Gigartinales, Rhodophyta). *J. Appl. Phycol*. 27:2405-2417.
867 Nauer, F., Gurgel, C. F. D., Ayres-Ostrock, L. M., Plastino, E. M., & Oliveira, M. C. 2019.
868 Phylogeography of the *Hypnea musciformis* species complex (Gigartinales, Rhodophyta)
869 with the recognition of cryptic species in the western Atlantic Ocean. *J. Phycol*. DOI:
870 10.1111/jpy.12848
871 Nei, M. & Li, W. H. 1979. Mathematical model for studying genetic variation in terms of restriction
872 endonucleases. *Proc. Natl. Acad. Sci.* 76:5269-5273.
873 Nei, M. 1978. Estimation of average heterozygosity and genetic distance from a small number of
874 individuals. *Genetics*. 89:583-590.
875 Neiva, J., Assis, J., Fernandes, F., Pearson, G. A. & Serrão, E. A. 2014. Species distribution models
876 and mitochondrial DNA phylogeography suggest an extensive biogeographical shift in the
877 high-intertidal seaweed *Pelvetia canaliculata*. *J. Biogeogr.* 41:1137-1148.
878 Neiva, J., Serrão, E. A., Assis, J., Pearson, G. A., Coyer, J. A., Olsen, J. L., Hoarau, G. & Valero, M.
879 2016. Climate oscillations, range shifts and phylogeographic patterns of North Atlantic
880 Fucaceae. *In* Zi-Min, H. & Ceridwen, F. [Eds.] *Seaweed Phylogeography*. Springer,
881 Dordrecht, pp. 279-308.

882 Nguyen, L. T., Schmidt, H. A., von Haeseler, A. & Minh, B. Q. 2014. IQ-TREE: a fast and effective
883 stochastic algorithm for estimating maximum-likelihood phylogenies. *Mol. Biol. Evol.*
884 32:268-274.
885 Nicastro, K. R., Zardi, G. I., Teixeira, S., Neiva, J., Serrão, E. A. & Pearson, G. A. 2013. Shift
886 happens: trailing edge contraction associated with recent warming trends threatens a distinct
887 genetic lineage in the marine macroalga *Fucus vesiculosus. BMC Biol.* 11:6.
888 Ocaranza-Barrera, P., González-Wevar, C. A, Guillemin, M-L., Rosenfeld, S. & Mansilla, A. 2018.
889 Molecular divergence between *Iridaea cordata* (Turner) Bory de Saint-Vincent 1826
890 populations from Antarctic Peninsula and the Magellan Region. *J. Appl. Phycol.*
891 doi.org/10.1007/s10811-018-1656-2
892 Palumbi, S. R. 2003 Population genetics, demographic connectivity, and the design of marine
893 reserves. *Ecol. Appl.* 13:S146-S158.
894 Peakall, R. O. D. & Smouse, P. E. 2006. GENALEX 6: genetic analysis in Excel. Population genetic
895 software for teaching and research. *Mol. Ecol. Res.* 6:288-295.
896 Pellegrino, K. C., Rodrigues, M. T., Waite, A. N., Morando, M., Yassuda, Y. Y. & Sites Jr, J. W.
897 2005. Phylogeography and species limits in the *Gymnodactylus darwinii* complex
898 (Gekkonidae, Squamata): genetic structure coincides with river systems in the Brazilian
899 Atlantic Forest. *Biol. J. Linnean Soc.* 85:13-26.
900 Peluso, L., Tascheri, V., Nunes, F. L. D., Castro, C. B., Pires, D. O. & Zilberberg, C. 2018.
901 Contemporary and historical oceanographic processes explain genetic connectivity in a
902 Southwestern Atlantic coral. *Sci. Rep.* 8:2684.
903 Pereyra, R. T., Bergström, L., Kautsky, L. & Johannesson, K. 2009. Rapid speciation in a newly
904 opened postglacial marine environment, the Baltic Sea. *BMC Evol. Biol.* 9:70.

905 Pil, M. W., Boeger, M. R., Muschner, V. C., Pie, M. R., Ostrensky, A. & Boeger, W. A. 2011.
906 Postglacial north–south expansion of populations of *Rhizophora mangle* (Rhizophoraceae)
907 along the Brazilian coast revealed by microsatellite analysis. *Am. J. Bot.* 98:1031-1039.
908 Pinheiro, H. T., Bernardi, G., Simon, T., Joyeux, J. C., Macieira, R. M., Gasparini, J. L., Rocha, C. &
909 Rocha, L. A. 2017. Island biogeography of marine organisms. *Nature*. 549:82-85.
910 Piry, S., Luikart, G. & Cornuet, J. M. 1999. Computer note. BOTTLENECK: a computer program
911 for detecting recent reductions in the effective size using allele frequency data. *J. Hered.*
912 90:502-503.
913 Plastino, E. M. & Oliveira, E. C. 1997. *Gracilaria caudata* J. Agardh (Gracilariales, Rhodophyta) -
914 restoring an old name for a common western Atlantic alga. *Phycologia*. 36:225-232.
915 Prates, A. P., Henrique De Lima, L. & Chatwin, A. 2007. Coastal and marine conservation priorities
916 in Brazil. *Priorities for coastal and marine conservation in South America*.
917 *ArlingtonVirginia. USA: The Nature Conservancy*, 15-23.
918 Pritchard, J. K., Stephens, M. & Donnelly, P. 2000. Inference of population structure using
919 multilocus genotype data. *Genetics.* 155:945-959.
920 Rocha, L. A. 2003. Patterns of distribution and processes of speciation in Brazilian reef fishes. *J.*
921 *Biogeogr.* 30:1161-1171.
922 Rosenberg, N. A. 2004. DISTRUCT: a program for the graphical display of population structure.
923 *Mol. Ecol. Notes*. 4:137-138.
924 Saada, G., Nicastro, K. R., Jacinto, R., McQuaid, C. D., Serrao, E. A., Pearson, G. A. & Zardi, G. I.
925 2016. Taking the heat: distinct vulnerability to thermal stress of central and threatened
926 peripheral lineages of a marine macroalga. *Divers. Distrib.* 22:1060-1068.
927 Santos, S., Hrbek, T., Farias, I. P., Schneider, H. & Sampaio, I. 2006. Population genetic structuring
928 of the king weakfish, *Macrodon ancylodon* (Sciaenidae), in Atlantic coastal waters of South
929 America: deep genetic divergence without morphological change. *Mol. Ecol.* 15:4361-4373.

930 Saunders, G. W. 2005. Applying DNA barcoding to red macroalgae: a preliminary appraisal holds
931 promise for future applications. *Philos. Trans. R. Soc. Lond. B. Biol. Sci.* 360:1879-1888.
932 Schmid, C., Schäfer, H., Zenk, W. & Podestá, G. 1995. The Vitória eddy and its relation to the Brazil
933 Current. *J. Phys. Oceanogr.* 25:2532-2546.
934 Suguio, K., Martin, L., Bittencourt, A. C. D. S. P., Dominguez, J. M. L., Flexor, J. & Azevedo, O. E.
935 G. 1985. Flutuações do nível relativo do mar durante o Quaternário Superior ao longo do
936 litoral brasileiro e suas implicações na sedimentação costeira. *Braz. J. Geol.* 15:273-286.
937 Tajima, F. 1989. Statistical method for testing the neutral mutation hypothesis by DNA
938 polymorphism. *Genetics*. 123:585-595.
939 Tamura, K., Peterson, D., Peterson, N., Stecher, G., Nei, M. & Kumar, S. 2011. MEGA5: molecular
940 evolutionary genetics analysis using maximum likelihood, evolutionary distance, and
941 maximum parsimony methods. *Mol. Biol. Evol.* 28:2731-2739.
942 Tellier, F., Meynard, A. P., Correa, J. A., Faugeron, S. & Valero, M. 2009. Phylogeographic analyses
943 of the 30° S south-east Pacific biogeographic transition zone establish the occurrence of a
944 sharp genetic discontinuity in the kelp *Lessonia nigrescens*: Vicariance or parapatry? *Mol.*
945 *Phylogenetics Evol.* 53:679-693.
946 Tellier, F., Tapia, J., Faugeron, S., Destombe, C. & Valero, M. 2011. The *Lessonia nigrescens*
947 species complex (Laminariales, Phaeophyceae) shows strict parapatry and complete
948 reproductive isolation in a secondary contact zone. *J. Phycol.* 47:894-903.
949 Thomé, M. T. C., Zamudio, K. R., Haddad, C. F. & Alexandrino, J. 2014. Barriers, rather than
950 refugia, underlie the origin of diversity in toads endemic to the Brazilian Atlantic Forest.
951 *Mol. Ecol.* 23:6152-6164.
952 Trigueiro, T. G., Pereira, D. C., Martins, A. P., Colepicolo, P. & Marinho-Soriano, E. 2017.
953 Cultivation of three color strains of *Gracilaria domingensis* in an integrated organic system.
954 *Int. Aquatic Res.* 9:225-233.

Ursi, S., Pedersén, M., Plastino, E. & Snoeijs, P. 2003. Intraspecific variation of photosynthesis, respiration and photoprotective carotenoids in *Gracilaria birdiae* (Gracilariales: Rhodophyta). *Mar. Biol.* 142:997-1007.

Valero, M., Guillemin, M. L., Destombe, C., Jacquemin, B., Gachon, C. M., Badis, Y., Buschmann, A. H., ... Faugeron, S. 2017. Perspectives on domestication research for sustainable seaweed aquaculture. *Perspect. Phycol.* 4:33-46.

van Oosterhout, C., Hutchinson, W. F., Wills, D. P. & Shipley, P. 2004. MICRO-CHECKER: software for identifying and correcting genotyping errors in microsatellite data. *Mol. Ecol. Notes.* 4:535-538.

Waples, R. S., Punt, A. E. & Cope, J. M. 2008. Integrating genetic data into management of marine resources: how can we do it better? *Fish Fish*. 9:423-449.

Weir, B. S. & Cockerham, C. C. 1984. Estimating *F*-statistics for the analysis of population structure. *Evolution*. 38:1358-1370.

Yokoya, N.S. & Oliveira, E.C. 1992. Effects of salinity on the growth rate, morphology and water content of some Brazilian red alga of economic importance. *Cienc. Mar.* 18:49-64.

Zuccarello, G. C., Burger, G., West, J. A. & King, R. J. 1999. A mitochondrial marker for red algal intraspecific relationships. *Mol. Ecol.* 8:1443-1447.

DATA ACCESSIBILITY STATEMENT

Microsatellite genotypes will be deposited for free access in DRYAD.

TABLE 1 Sampling sites for *Gracilaria caudata* and their genetic diversity for two mitochondrial markers (COI and *cox*2-3) in Brazil. Molecular diversity estimates calculated for COI (630 bp) and *cox*2-3 (358 bp): number of sequences (N), number of haplotypes (nH), gene diversity (H), nucleotide diversity (π), number of polymorphic sites (S), Tajima's *D* (D) and Fu's F_S (F_S) statistics. Standard deviation (SD) is given in parentheses. Ceará (CE), Rio Grande do Norte (RN), Paraíba (PB), Pernambuco (PE), Bahia (BA), Espírito Santo (ES) and São Paulo (SP). North-eastern haplogroup: CE, RN, PB and PE; BA and south-eastern haplogroup: BA, ES and SP. All specimens were collected in-between high and low intertidal areas uncovered at low tide

Site (State)	Coordinates (GPS)	COI							*cox*2-3						
		N	nH	H (SD)	π (*10^{-2}) (SD)	S	D	F_S	N	nH	H (SD)	π (*10^{-2}) (SD)	S	D	F_S
CE	03º24'36.0"S/39º01'50.0"W	26	10	0.750 (0.074)	0.270 (0.182)	12	-1.542*	-4.389**	24	2	0.463 (0.069)	0.129 (0.131)	1	1,231	1,362
RN	05º15'41.0"S/35º23'11.0"W	22	5	0.649 (0.064)	0.220 (0.157)	6	-0.482	-0.145	19	3	0.374 (0.129)	0.153 (0.147)	2	-0.094	-0.071
PB	07º 17'62.9"S/34 º 48'08.5"W	22	5	0.528 (0.118)	0.186 (0.138)	5	-0.430	-0.582	22	2	0.311 (0.106)	0.087 (0.103)	1	0.236	0.647
PE	08º07'58.9"S/34º53'57.3"W	23	4	0.557 (0.083)	0.173 (0.131)	4	0.018	0.347	22	3	0.536 (0.090)	0.232 (0.192)	3	0.025	0.890
BA	12º44'28.0"S/38º09'01.0"W	23	4	0.525 (0.094)	0.097 (0.089)	3	-0.615	-0.964	20	4	0.363 (0.130)	0.230 (0.001)	4	-0.773	-0.443
ES	20º48'31.0"S/40º36'39.0"W	23	2	0.087 (0.077)	0.027 (0.042)	2	-1.514*	-0.153	18	1	0.000 (0.000)	0.000 (0.000)	0	0.000	0.000
SP	23º55'01.0"S/46º19'16.8"W	18	1	0.000 (0.000)	0.000 (0.000)	0	0.000	0.000	19	1	0.000 (0.000)	0.000 (0.000)	0	0.000	0.000
	Total *G. caudata*	157	21	0.442 (0.073)	0.139 (0.106)	21	-0.652	-0.841	144	6	0.292 (0.075)	0.119 (0.109)	5	0.089	0.340
	North-eastern haplogroup	93	16	0.621 (0.085)	0.212 (0.152)	16	-0.609	-1,192	87	4	0.421 (0.099)	0.150 (0.143)		0.350	0.707
	BA + south-eastern haplogroup	41	5	0.204 (0.057)	0.041 (0.043)	5	-0.710	-0.558	37	3	0.121 (0.043)	0.076 (0.064)		-0.257	-0.443

*p< 0.05; **p< 0.001

TABLE 2 (a) Pairwise estimates of genetic differentiation (F_{ST}) between the seven sampled *Gracilaria caudata* sites for COI (below the diagonal) and *cox*2-3 (above the diagonal) and (b) analysis of molecular variance (AMOVA) within sites, among sites within haplogroup and among haplogroups for both molecular markers. Haplogroups were defined according to the haplotype network (see Figure 3; north-eastern haplogroup: CE, RN, PB and PE; Bahia and south-eastern haplogroup: BA, ES and SP). Ceará (CE), Rio Grande do Norte (RN), Paraíba (PB), Pernambuco (PE), Bahia (BA), Espírito Santo (ES) and São Paulo (SP). Degrees of freedom (d.f.) and sum of squares (SS).

(a)

	CE	RN	PB	PE	BA	ES	SP
CE		0.004	0.357**	0.111*	0.701**	0.887**	0.922**
RN	-0.020		0.460**	0.199**	0.674**	0.878**	0.917**
PB	0.209**	0.155*		0.039	0.776**	0.939**	0.956**
PE	0.259**	0.211**	0.003		0.628**	0.815**	0.871**
BA	0.636**	0.690**	0.723**	0.727**		0.073	0.709**
ES	0.804**	0.850**	0.870**	0.874**	0.834**		1.000**
SP	0.805**	0.852**	0.875**	0.879**	0.856**	0.948**	

*p< 0.05; **p< 0.001

(b)

Source of variation	COI				
	d.f.	SS	Variance components	% variation	p-value
Among haplogroups	1	108.348	1.291	58.72	p< 0.05
Among localities within haplogroups	5	52.510	0.448	20.38	p< 0.000
Within localities	150	68.912	0.459	20.90	p< 0.000
Total	156	229.771	2.198	-	-
	*cox*2-3				
	d.f.	SS	Variance components	% variation	p-value
Among haplogroups	1	70.336	0.967	71.22	p< 0.05
Among localities within haplogroups	5	18.742	0.171	12.60	p< 0.001
Within localities	137	30.131	0.219	16.18	p< 0.001
Total	143	119.208	1.359	-	-

TABLE 3 Genetic diversity of *Gracilaria caudata* calculated for 15 nuclear microsatellite loci. For each site, the number of individuals genotyped is indicated (n). Multi-locus mean estimates of the number of alleles per locus (N_a), expected heterozygosity (H_e), observed heterozygosity (H_o), allele richness (A_R), frequency of private alleles (F_{PRIV}) and deviation from random mating (F_{IS}). F_{IS} values significantly different from zero are shown in bold. Standard deviation (SD) is given in parentheses. Ceará (CE), Rio Grande do Norte (RN), Paraíba (PB), Pernambuco (PE), Bahia (BA), Espírito Santo (ES) and São Paulo (SP). Haplogroups were defined using the mitochondrial data set. North-eastern haplogroup: CE, RN, PB and PE; BA and south-eastern haplogroup: BA, ES and SP.

Site (State)	Coordinates (GPS)	Microsatellite Loci						
		n	N_a	H_e (SD)	H_o (SD)	F_{IS}	A_R	F_{PRIV}
CE	03º24'36.0"S/ 39º01'50.0"W	72	4.267	0.379 (0.248)	0.384 (0.282)	-0.006	3.803	0.047
RN	05º15'41.0"S/ 35º23'11.0"W	52	5.267	0.458 (0.249)	0.479 (0.280)	-0.037	4.992	0.076
PB	07º17'62.9"S/ 34º48'08.5"W	79	4.533	0.386 (0.242)	0.402 (0.298)	-0.034	4.077	0.103
PE	08º07'58.9"S/ 34º53'57.3"W	53	4.000	0.366 (0.272)	0.379 (0.296)	-0.027	3.780	0.067
BA	12º44'28.0"S/ 38º09'01.0"W	55	3.933	0.333 (0.275)	0.298 (0.250)	**0.115**	3.692	0.068
ES	20º48'31.0"S/ 40º36'39.0"W	51	3.733	0.345 (0.301)	0.392 (0.376)	**-0.125**	3.582	0.196
SP	23º55'01.0"S/ 46º19'16.8"W	49	3.400	0.284 (0.279)	0.288 (0.309)	-0.001	3.299	0.157

Total *G. caudata*	411	4.162	0.364 (0.267)	0.375 (0.299)	-0.016	3.889	-
North-eastern haplogroup	256	4.517	0.446 (0.256)	0.407 (0.266)	-0.026	4.163	0.073
BA + south-eastern haplogroup	155	3.576	0.363 (0.329)	0.340 (0.323)	-0.063	3.440	0.177

TABLE 4 Genetic variability within the sampled sites of *Gracilaria caudata.* For each site and each locus, the number of individuals genotyped (n) is indicated. The number of alleles per locus (N_a), expected heterozygosity (H_e), observed heterozygosity (H_o), frequency of private alleles (Freq. N_{priv}) and estimates of deviation from random mating (F_{IS}) was calculated for the 15 selected microsatellite loci independently. F_{IS} values significantly different from zero are shown in bold. Presence of null allele frequency was tested with MICRO-CHECKER software (Oosterhout et al. 2004) and loci for which frequency of null alleles was significant are indicated. Mean and standard error (SE) computed over the 15 loci are given in parentheses.

	Ceará (CE)					Rio Grande do Norte (RN)					Paraíba (PB)					Pernambuco (PE)				
Loci	n	Na	Ho	He	F_{IS}	n	Na	Ho	He	F_{IS}	n	Na	Ho	He	F_{IS}	N	Na	Ho	He	F_{IS}
GraC_01	69	8	0.725	0.611	-0.180	46	6	0.413	0.371	-0.101	76	8	0.592	0.564	-0.008	51	7	0.490	0.413	-0178
GraC_02	57	4	0.684	0.582	-0.168	46	5	0.804	0.683	-0.167	70	6	0.329	0.333	0.096	48	3	0.354	0.295	-0.191
GraC_03	70	4	0.757	0.594	-0.250	52	7	0.808	0.584	-0.376	77	6	0.935	0.601	-0.508*	51	8	0.961	0.615	-0.556
GraC_04	60	10	0.733	0.776	0.069	49	16	0.837	0.809	-0.024	79	9	0.671	0.682	0.032	48	10	0.479	0.838	0.437*
GraC_05	72	4	0.583	0.579	-0.024	48	5	0.479	0.479	0.011	79	6	0.532	0.588	0.142	53	4	0.528	0.596	0.123
GraC_06	64	4	0.219	0.395	0.479*	49	4	0.653	0.586	-0.103	79	6	0.203	0.402	0.468*	53	4	0.377	0.474	0.212*
GraC_07	71	6	0.634	0.612	-0.028	50	8	0.800	0.794	0.003	77	7	0.818	0.639	-0.268	48	7	0.854	0.717	-0.181
GraC_08	72	3	0.222	0.220	-0.001	47	5	0.426	0.473	0.112	75	3	0.107	0.102	-0.043	48	1	0.000	0.000	-
GraC_10	68	1	0.000	0.000	-	50	1	0.000	0.000	-	68	1	0.000	0.000	-	48	1	0.000	0.000	-
GraC_12	68	2	0.191	0.336	0.436*	49	3	0.367	0.490	0.260	77	2	0.545	0.486	-0.097	52	2	0.288	0.299	0.044
GraBC_01	72	4	0.056	0.054	-0.012	51	3	0.275	0.294	0.076	79	3	0.316	0.326	0.095	53	2	0.170	0.155	-0.083
GraBC_02	72	5	0.181	0.180	0.006	52	5	0.269	0.261	-0.021	79	2	0.013	0.013	0.665	53	3	0.075	0.073	-0.022
GraBC_03	71	2	0.014	0.014	-0.000	51	2	0.098	0.093	-0.042	77	2	0.000	0.026	0.665	51	2	0.020	0.019	0.000
GraBC_04	72	3	0.486	0.467	-0.035	51	4	0.745	0.729	-0.013	75	3	0.547	0.520	-0.041	49	2	0.592	0.487	-0.206
GraBC_05	72	4	0.278	0.265	-0.043	51	5	0.216	0.216	0.010	76	4	0.421	0.513	0.229	52	4	0.500	0.507	0.024
Mean over loci**			0.384	0.379	-0.006			0.479	0.457	-0.037			0.400	0.396	-0.034			0.379	0.365	-0.027
(SE)**			(0.283)	(0.249)				(0.279)	(0.249)				(0.293)	(0.241)				(0.296)	(0.272)	
Freq. Npriv		0.047					0.076					0.103					0.067			

* Probable null alleles

** Calculated without the locus presenting null alleles

	Bahia (BA)					Espírito Santo (ES)					São Paulo (SP)				
Loci	n	Na	Ho	He	F_{IS}	n	Na	Ho	He	F_{IS}	n	Na	Ho	He	F_{IS}
GraC_01	53	5	0.396	0.446	0.120	51	5	0.471	0.386	-0.210	48	5	0.438	0.421	-0.029
GraC_02	51	3	0.118	0.112	-0.043	43	2	0.186	0.169	-0.091	39	2	0.462	0.355	-0.288
GraC_03	53	5	0.698	0.741	0.064	44	5	0.955	0.702	-0.354	45	3	0.600	0.586	0.022
GraC_04	53	12	0.547	0.689	0.212*	51	9	0.627	0.693	0.122	45	14	0.667	0.844	0.210*
GraC_05	55	6	0.636	0.655	0.044	48	6	0.646	0.672	0.072*	47	4	0.532	0.545	0.031
GraC_06	55	5	0.473	0.512	0.091	51	5	0.941	0.711	-0.322	47	5	0.383	0.531	0.266*
GraC_07	54	5	0.630	0.610	-0.014	49	6	0.714	0.671	-0.084	46	3	0.109	0.178	0.401
GraC_08	54	3	0.037	0.037	-0.005	50	2	0.020	0.020	-0.000	48	2	0.021	0.021	0.000
GraC_10	52	2	0.212	0.189	-0.109	46	2	0.196	0.177	-0.098	42	1	0.000	0.000	-*
GraC_12	54	2	0.222	0.499	0.561*	50	1	0.000	0.000	-	47	2	0.000	0.042	1.000
GraBC_01	55	1	0.000	0.000	-	51	2	0.078	0.075	-0.031	47	2	0.021	0.021	-0.000
GraBC_02	54	3	0.333	0.350	0.060	51	1	0.000	0.000	-	48	2	0.083	0.080	-0.032
GraBC_03	55	2	0.018	0.018	-0.000	51	3	0.098	0.130	0.411	49	1	0.000	0.000	-
GraBC_04	54	2	0.019	0.018	0.000	51	4	0.922	0.654	-0.401	48	3	0.958	0.562	-0.699
GraBC_05	54	3	0.130	0.123	-0.042	50	3	0.020	0.114	0.828	49	2	0.041	0.078	0.487
Mean over loci**			0.296	0.332	**0.115**			0.391	0.347	**-0.125**			0.289	0.286	-0.001
(SE)**			(0.248)	(0.274)				(0.377)	(0.300)				(0.310)	(0.286)	
Freq. Npriv		0.068					0.196					0.157			

* Probable null alleles

** Calculated without the locus presenting null alleles

TABLE 5 (a) Pairwise estimates of genetic differentiation (F_{ST}) between the seven sampled *Gracilaria caudata* sites for the 15 selected microsatellite loci and (b) analysis of molecular variance (AMOVA) within sites, among sites within haplogroup and among haplogroups for the nuclear microsatellite markers. Haplogroups were defined according to the haplotype network (see Figure 3, north-eastern haplogroup: CE, RN, PB and PE; BA and south-eastern haplogroup: BA, ES and SP). Ceará (CE), Rio Grande do Norte (RN), Paraíba (PB), Pernambuco (PE), Bahia (BA), Espírito Santo (ES) and São Paulo (SP). Degrees of freedom (d.f.) and sum of squares (SS).

(a)

	CE	RN	PB	PE	BA	ES	SP
CE							
RN	0.173*						
PB	0.140*	0.217*					
PE	0.085*	0.204*	0.038*				
BA	0.309*	0.393*	0.303*	0.297*			
ES	0.449*	0.456*	0.420*	0.447*	0.299*		
SP	0.477*	0.477*	0.417*	0.463*	0.381*	0.228*	

*p <0.001

(b)

Source of variation	Microsatellites				
	d.f.	SS	Variance components	% variation	p-value
Among haplogroups	1	483.370	1.081	29.34	p< 0.05
Among localities within haplogroups	5	335.866	0.555	15.07	p< 0.001
Within localities	815	1670.016	2.049	55.58	p< 0.001
Total	821	2489.252	3.686	-	-

FIGURE 1 Map of the Brazilian coast showing the direction of major ocean currents: North Brazil Current (NBC), South Equatorial Current (SEC), Brazil Current (BC) and the South Atlantic Central Waters (SACW). Gyres appear as dashed lines. Known biogeographical barriers, such as the Vitória-Trindade Ridge, the Doce and the São Francisco river mouths are indicated. Sampling sites are shown (black dots): CE, Ceará (03º24'36"S/39º01'50"W); RN, Rio Grande do Norte (05º15'41.0"S/35º23'11.0"W); PB, Paraíba (07°17'62.9"S/34°48'08.5"W); PE, Pernambuco (08º07'58.9"S/34º53'57.3"W); BA, Bahia (12º44'28.0"S/38º09'01.0"W); ES, Espírito Santo (20º48'31.0"S/40º36'39.0"W); and SP, São Paulo (23º55'01.0"S/46º19'16.8"W). Diagram of the main marine currents and oceanic features based on Santos et al. (2006), Arruda et al. (2013), Mill et al. (2015) and Peluso et al. (2018). Green shaded areas indicate terrestrial coastal refugia and their boundaries, redrawn from the most historically stable Atlantic forest areas proposed in Carnaval and Moritz (2008). Please note that the number and localization of refugia predicted for the Brazilian Atlantic forest south of the Doce River was not as well defined as for the northern part of the coast (Carnaval & Moritz 2008) and that the existence of three main refugia have been proposed: 1) Pernambuco (i.e., PE), 2) Bahia (i.e., BA) and 3) a small refuge with a localization difficult to predict that could be at the boundaries of the states of Espírito Santo and Rio de Janeiro (i.e., ES+SP); the last refugium corresponding to a unique center of endemism identified for mammals, birds, butterflies and plants.

FIGURE 2 Maximum likelihood (ML) trees based on: (a) *rbc*L data and (b) concatenated mtDNA haplotypes (COI and *cox*2-3 spacer) from distinct populations of *Gracilaria caudata* along the Brazilian coast. *Gracilaria birdiae* was used as outgroup. Bootstrap values for 2000 replicates are indicated on branches. Sequences from GenBank are followed by their accession number. New sequences produced in this study for *rbc*L are shown in bold. Sites of *G. caudata* sampled: Ceará (CE), Rio Grande do Norte (RN), Paraíba (PB), Pernambuco (PE), Bahia (BA), Espírito Santo (ES),

São Paulo (SP) and Santa Catarina (SC) States. North-eastern (NE), south-eastern (SE) and southern (S) populations. The number of sequences corresponding to each haplotype is given in parentheses.

FIGURE 3 Genetic sub-divisions of *Gracilaria caudata* observed using concatenated mtDNA haplotypes (COI and *cox*2-3 spacer) and 15 selected microsatellite loci. (a) Pie charts show the geographical distribution of haplotypes; the number of sequences amplified for each population is given in parentheses. The pie chart colour code corresponds to that used in the haplotype network. (b) Median-joining haplotype network. In the network, each circle represents a haplotype and its size is proportional to the frequency at which the haplotype was encountered in each site. Black squares represent hypothetical un-sampled haplotypes and number of mutations corresponds to number of segments between two haplotypes. (c) Bayesian analysis using STRUCTURE for the seven studied populations of *G. caudata*. Each horizontal bar represents a different individual. Each colour represents the proportion of individual genome assigned to each genetic group (K). Individuals are ordered geographically from the north-east to the south-east. The bar plot on the left gives results obtained in STRUCTURE when all seven sampled populations were analysed together and the bar plot on the right gives results obtained for the two main clusters analysed independently. When including all sampled populations, the best fitting number of clusters was K =2 (north-east, NE vs. Bahia plus the south-east, BA+SE). Within each main cluster, the best fitting number of clusters was K =3. Ceará (CE), Rio Grande do Norte (RN), Paraíba (PB), Pernambuco (PE), Bahia (BA), Espírito Santo (ES) and São Paulo (SP).

FIGURE 4 Allele frequency distributions for the three microsatellite loci GraC_03, GraC_12 and GraBC_01 observed in each of the seven studied *Gracilaria caudata* sites. Sites on the y–axis are ordered from north to south. Numbers on the x-axis are allele sizes in base pairs for each locus. Each circle indicates the presence of the corresponding allele; the diameter of the circle represents the

frequency of that allele in the population. North-eastern (NE) and Bahia plus the south-eastern (BA+SE) sites: Ceará (CE), Rio Grande do Norte (RN), Paraíba (PB), Pernambuco (PE), Bahia (BA), Espírito Santo (ES) and São Paulo (SP).

FIGURE S1 Mantel test of the relationship between genetic and geographic distances, using the mitochondrial markers (a) COI and (b) *cox*2-3, for the seven sampled *Gracilaria caudata* localities along the Brazilian coast, expressed as F_{ST} versus the distance in kilometres (km). The F_{ST} values calculated among the locations from the north-east (NE) region (Ceará, Rio Grande do Norte, Paraíba and Pernambuco) are in red. The F_{ST} values calculated between the Bahia (BA) region and NE are in blue. The F_{ST} values calculated among the locations from the south-east (SE) region (São Paulo and Espírito Santo) and NE and BA are in black.

FIGURE S2 Mantel test of the relationship between genetic and geographic distance, using nuclear microsatellite markers, for the seven sampled *Gracilaria caudata* localities along the Brazilian coast, expressed as F_{ST} versus the distance in kilometres (km). The F_{ST} values calculated among the locations from the north-east (NE) region (Ceará, Rio Grande do Norte, Paraíba and Pernambuco) are in red. The F_{ST} values calculated between the Bahia (BA) region and NE are in blue. The F_{ST} values calculated among the locations from the south-east (SE) region (São Paulo and Espírito Santo) and NE and BA are in black.

FIGURE S3 Discriminant analysis of principal components (DAPC) showing the seven sampled *Gracilaria caudata* localities grouped into six genetic clusters. Ceará (CE), Rio Grande do Norte (RN), Paraíba (PB), Pernambuco (PE), Bahia (BA), Espírito Santo (ES) and São Paulo (SP).

Site (State)	Coordinates (GPS)	COI							*cox2*-3						
		N	nH	H (SD)	π (*10^{-2}) (SD)	S	D	F_S	N	nH	H (SD)	π (*10^{-2}) (SD)	S	D	F_S
CE	03º24'36.0"S/39º01'50.0"W	26	10	0.750 (0.074)	0.270 (0.182)	12	-1.542*	-4.389**	24	2	0.463 (0.069)	0.129 (0.131)	1	1,231	1,362
RN	05º15'41.0"S/35º23'11.0"W	22	5	0.649 (0.064)	0.220 (0.157)	6	-0.482	-0.145	19	3	0.374 (0.129)	0.153 (0.147)	2	-0.094	-0.071
PB	07º17'62.9"S/34º48'08.5"W	22	5	0.528 (0.118)	0.186 (0.138)	5	-0.430	-0.582	22	2	0.311 (0.106)	0.087 (0.103)	1	0.236	0.647
PE	08º07'58.9"S/34º53'57.3"W	23	4	0.557 (0.083)	0.173 (0.131)	4	0.018	0.347	22	3	0.536 (0.090)	0.232 (0.192)	3	0.025	0.890
BA	12º44'28.0"S/38º09'01.0"W	23	4	0.525 (0.094)	0.097 (0.089)	3	-0.615	-0.964	20	4	0.363 (0.130)	0.230 (0.001)	4	-0.773	-0.443
ES	20º48'31.0"S/40º36'39.0"W	23	2	0.087 (0.077)	0.027 (0.042)	2	-1.514*	-0.153	18	1	0.000 (0.000)	0.000 (0.000)	0	0.000	0.000
SP	23º55'01.0"S/46º19'16.8"W	18	1	0.000 (0.000)	0.000 (0.000)	0	0.000	0.000	19	1	0.000 (0.000)	0.000 (0.000)	0	0.000	0.000
Total *G. caudata*		157	21	0.442 (0.073)	0.139 (0.106)	21	-0.652	-0.841	144	6	0.292 (0.075)	0.119 (0.109)	5	0.089	0.340
North-eastern haplogroup		93	16	0.621 (0.085)	0.212 (0.152)	16	-0.609	-1,192	87	4	0.421 (0.099)	0.150 (0.143)		0.350	0.707
BA + south-eastern haplogroup		41	5	0.204 (0.057)	0.041 (0.043)	5	-0.710	-0.558	37	3	0.121 (0.043)	0.076 (0.064)		-0.257	-0.443

*p< 0.05; **p< 0.001

(a)

	CE	RN	PB	PE	BA	ES	SP
CE		0.004	0.357**	0.111*	0.701**	0.887**	0.922**
RN	-0.020		0.460**	0.199**	0.674**	0.878**	0.917**
PB	0.209**	0.155*		0.039	0.776**	0.939**	0.956**
PE	0.259**	0.211**	0.003		0.628**	0.815**	0.871**
BA	0.636**	0.690**	0.723**	0.727**		0.073	0.709**
ES	0.804**	0.850**	0.870**	0.874**	0.834**		1.000**
SP	0.805**	0.852**	0.875**	0.879**	0.856**	0.948**	

*p< 0.05; **p< 0.001

(b)

Source of variation	COI				
	d.f.	SS	Variance components	% variation	p-value
Among haplogroups	1	108.348	1.291	58.72	p< 0.05
Among localities within haplogroups	5	52.510	0.448	20.38	p< 0.000
Within localities	150	68.912	0.459	20.90	p< 0.000
Total	156	229.771	2.198	-	-
	*cox*2-3				
	d.f.	SS	Variance components	% variation	p-value
Among haplogroups	1	70.336	0.967	71.22	p< 0.05
Among localities within haplogroups	5	18.742	0.171	12.60	p< 0.001
Within localities	137	30.131	0.219	16.18	p< 0.001
Total	143	119.208	1.359	-	-

Site (State)	Coordinates (GPS)	Microsatellite Loci						
		n	N_a	H_e (SD)	H_o (SD)	F_{IS}	A_R	F_{PRIV}
CE	03º24'36.0"S/ 39º01'50.0"W	72	4.267	0.379 (0.248)	0.384 (0.282)	-0.006	3.803	0.047
RN	05º15'41.0"S/ 35º23'11.0"W	52	5.267	0.458 (0.249)	0.479 (0.280)	-0.037	4.992	0.076
PB	07º17'62.9"S/ 34º48'08.5"W	79	4.533	0.386 (0.242)	0.402 (0.298)	-0.034	4.077	0.103
PE	08º07'58.9"S/ 34º53'57.3"W	53	4.000	0.366 (0.272)	0.379 (0.296)	-0.027	3.780	0.067
BA	12º44'28.0"S/ 38º09'01.0"W	55	3.933	0.333 (0.275)	0.298 (0.250)	**0.115**	3.692	0.068
ES	20º48'31.0"S/ 40º36'39.0"W	51	3.733	0.345 (0.301)	0.392 (0.376)	**-0.125**	3.582	0.196
SP	23º55'01.0"S/ 46º19'16.8"W	49	3.400	0.284 (0.279)	0.288 (0.309)	-0.001	3.299	0.157
Total *G. caudata*		411	4.162	0.364 (0.267)	0.375 (0.299)	-0.016	3.889	-
North-eastern haplogroup		256	4.517	0.446 (0.256)	0.407 (0.266)	-0.026	4.163	0.073
BA + south-eastern haplogroup		155	3.576	0.363 (0.329)	0.340 (0.323)	-0.063	3.440	0.177

	Ceará (CE)					Rio Grande do Norte (RN)					Paraíba (PB)					Pernambuco (PE)				
Loci	n	Na	Ho	He	F_{IS}	n	Na	Ho	He	F_{IS}	n	Na	Ho	He	F_{IS}	N	Na	Ho	He	F_{IS}
GraC_01	69	8	0.725	0.611	-0.180	46	6	0.413	0.371	-0.101	76	8	0.592	0.564	-0.008	51	7	0.490	0.413	-0178
GraC_02	57	4	0.684	0.582	-0.168	46	5	0.804	0.683	-0.167	70	6	0.329	0.333	0.096	48	3	0.354	0.295	-0.191
GraC_03	70	4	0.757	0.594	-0.250	52	7	0.808	0.584	-0.376	77	6	0.935	0.601	-0.508*	51	8	0.961	0.615	-0.556
GraC_04	60	10	0.733	0.776	0.069	49	16	0.837	0.809	-0.024	79	9	0.671	0.682	0.032	48	10	0.479	0.838	0.437*
GraC_05	72	4	0.583	0.579	-0.024	48	5	0.479	0.479	0.011	79	6	0.532	0.588	0.142	53	4	0.528	0.596	0.123
GraC_06	64	4	0.219	0.395	0.479*	49	4	0.653	0.586	-0.103	79	6	0.203	0.402	0.468*	53	4	0.377	0.474	0.212*
GraC_07	71	6	0.634	0.612	-0.028	50	8	0.800	0.794	0.003	77	7	0.818	0.639	-0.268	48	7	0.854	0.717	-0.181
GraC_08	72	3	0.222	0.220	-0.001	47	5	0.426	0.473	0.112	75	3	0.107	0.102	-0.043	48	1	0.000	0.000	-
GraC_10	68	1	0.000	0.000	-	50	1	0.000	0.000	-	68	1	0.000	0.000	-	48	1	0.000	0.000	-
GraC_12	68	2	0.191	0.336	0.436*	49	3	0.367	0.490	0.260	77	2	0.545	0.486	-0.097	52	2	0.288	0.299	0.044
GraBC_01	72	4	0.056	0.054	-0.012	51	3	0.275	0.294	0.076	79	3	0.316	0.326	0.095	53	2	0.170	0.155	-0.083
GraBC_02	72	5	0.181	0.180	0.006	52	5	0.269	0.261	-0.021	79	2	0.013	0.013	0.665	53	3	0.075	0.073	-0.022
GraBC_03	71	2	0.014	0.014	-0.000	51	2	0.098	0.093	-0.042	77	2	0.000	0.026	0.665	51	2	0.020	0.019	0.000
GraBC_04	72	3	0.486	0.467	-0.035	51	4	0.745	0.729	-0.013	75	3	0.547	0.520	-0.041	49	2	0.592	0.487	-0.206
GraBC_05	72	4	0.278	0.265	-0.043	51	5	0.216	0.216	0.010	76	4	0.421	0.513	0.229	52	4	0.500	0.507	0.024
Mean over loci**			0.384	0.379	-0.006			0.479	0.457	-0.037			0.400	0.396	-0.034			0.379	0.365	-0.027
(SE)**			(0.283)	(0.249)				(0.279)	(0.249)				(0.293)	(0.241)				(0.296)	(0.272)	
Freq. Npriv		0.047					0.076					0.103					0.067			

* Probable null alleles

** Calculated without the locus presenting null alleles

	Bahia (BA)					Espírito Santo (ES)					São Paulo (SP)				
Loci	n	Na	Ho	He	F_{IS}	n	Na	Ho	He	F_{IS}	n	Na	Ho	He	F_{IS}
GraC_01	53	5	0.396	0.446	0.120	51	5	0.471	0.386	-0.210	48	5	0.438	0.421	-0.029
GraC_02	51	3	0.118	0.112	-0.043	43	2	0.186	0.169	-0.091	39	2	0.462	0.355	-0.288
GraC_03	53	5	0.698	0.741	0.064	44	5	0.955	0.702	-0.354	45	3	0.600	0.586	0.022
GraC_04	53	12	0.547	0.689	0.212*	51	9	0.627	0.693	0.122	45	14	0.667	0.844	0.210*
GraC_05	55	6	0.636	0.655	0.044	48	6	0.646	0.672	0.072*	47	4	0.532	0.545	0.031
GraC_06	55	5	0.473	0.512	0.091	51	5	0.941	0.711	-0.322	47	5	0.383	0.531	0.266*
GraC_07	54	5	0.630	0.610	-0.014	49	6	0.714	0.671	-0.084	46	3	0.109	0.178	0.401
GraC_08	54	3	0.037	0.037	-0.005	50	2	0.020	0.020	-0.000	48	2	0.021	0.021	0.000
GraC_10	52	2	0.212	0.189	-0.109	46	2	0.196	0.177	-0.098	42	1	0.000	0.000	-*
GraC_12	54	2	0.222	0.499	0.561*	50	1	0.000	0.000	-	47	2	0.000	0.042	1.000
GraBC_01	55	1	0.000	0.000	-	51	2	0.078	0.075	-0.031	47	2	0.021	0.021	-0.000
GraBC_02	54	3	0.333	0.350	0.060	51	1	0.000	0.000	-	48	2	0.083	0.080	-0.032
GraBC_03	55	2	0.018	0.018	-0.000	51	3	0.098	0.130	0.411	49	1	0.000	0.000	-
GraBC_04	54	2	0.019	0.018	0.000	51	4	0.922	0.654	-0.401	48	3	0.958	0.562	-0.699
GraBC_05	54	3	0.130	0.123	-0.042	50	3	0.020	0.114	0.828	49	2	0.041	0.078	0.487
Mean over loci**			0.296	0.332	**0.115**			0.391	0.347	**-0.125**			0.289	0.286	-0.001
(SE)**			(0.248)	(0.274)				(0.377)	(0.300)				(0.310)	(0.286)	
Freq. Npriv		0.068					0.196					0.157			

* Probable null alleles

** Calculated without the locus presenting null alleles

(a)

	CE	RN	PB	PE	BA	ES	SP
CE							
RN	0.173*						
PB	0.140*	0.217*					
PE	0.085*	0.204*	0.038*				
BA	0.309*	0.393*	0.303*	0.297*			
ES	0.449*	0.456*	0.420*	0.447*	0.299*		
SP	0.477*	0.477*	0.417*	0.463*	0.381*	0.228*	

*p <0.001

(b)

Source of variation	Microsatellites				
	d.f.	SS	Variance components	% variation	p-value
Among haplogroups	1	483.370	1.081	29.34	p< 0.05
Among localities within haplogroups	5	335.866	0.555	15.07	p< 0.001
Within localities	815	1670.016	2.049	55.58	p< 0.001
Total	821	2489.252	3.686	-	-

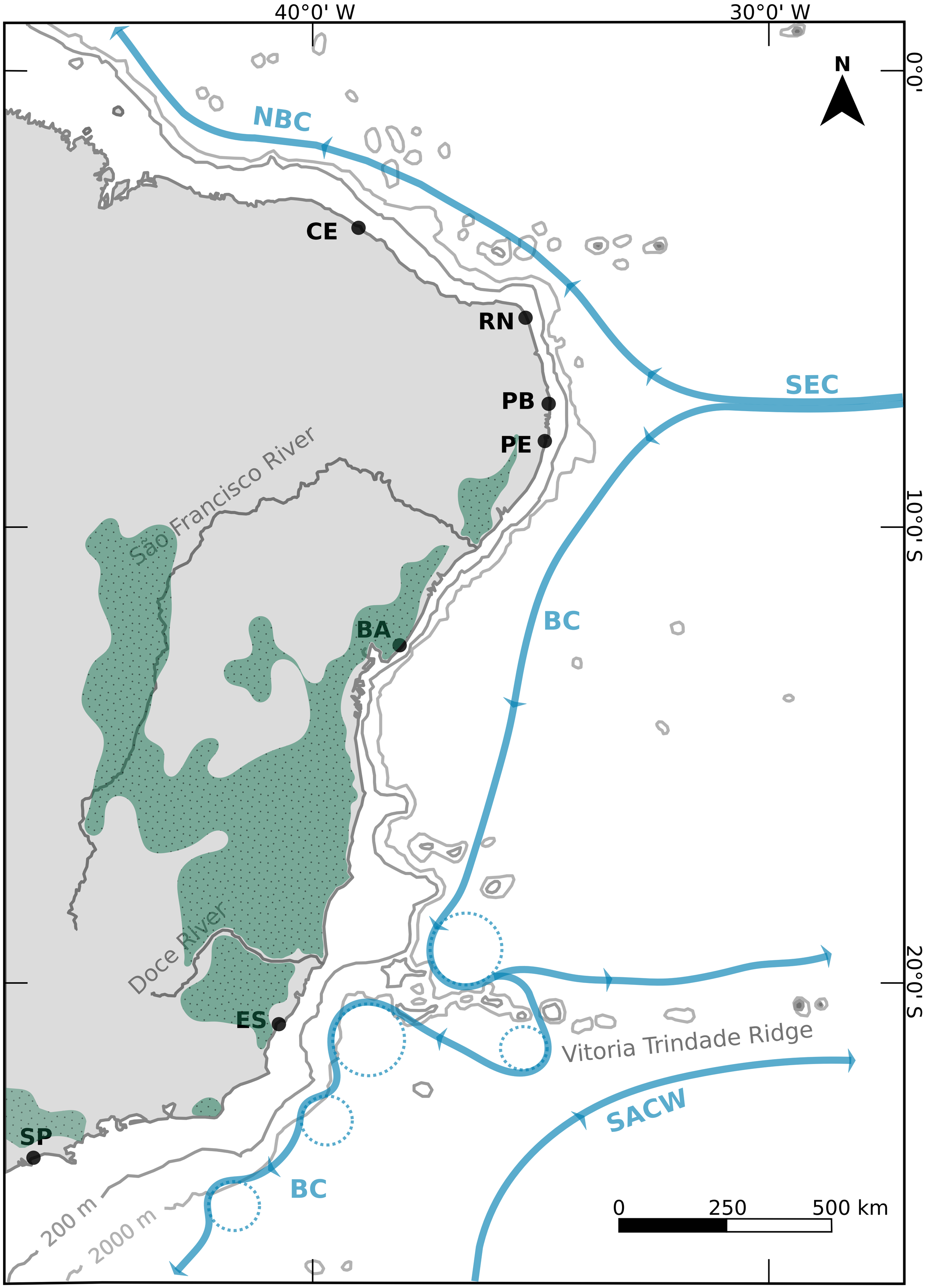
40°0' W
30°0' W
0°0'
10°0' S
20°0' S
N
NBC
SEC
BC
BC
SACW
CE
RN
PB
PE
BA
ES
SP
São Francisco River
Doce River
Vitoria Trindade Ridge
200 m
2000 m
0
250
500 km

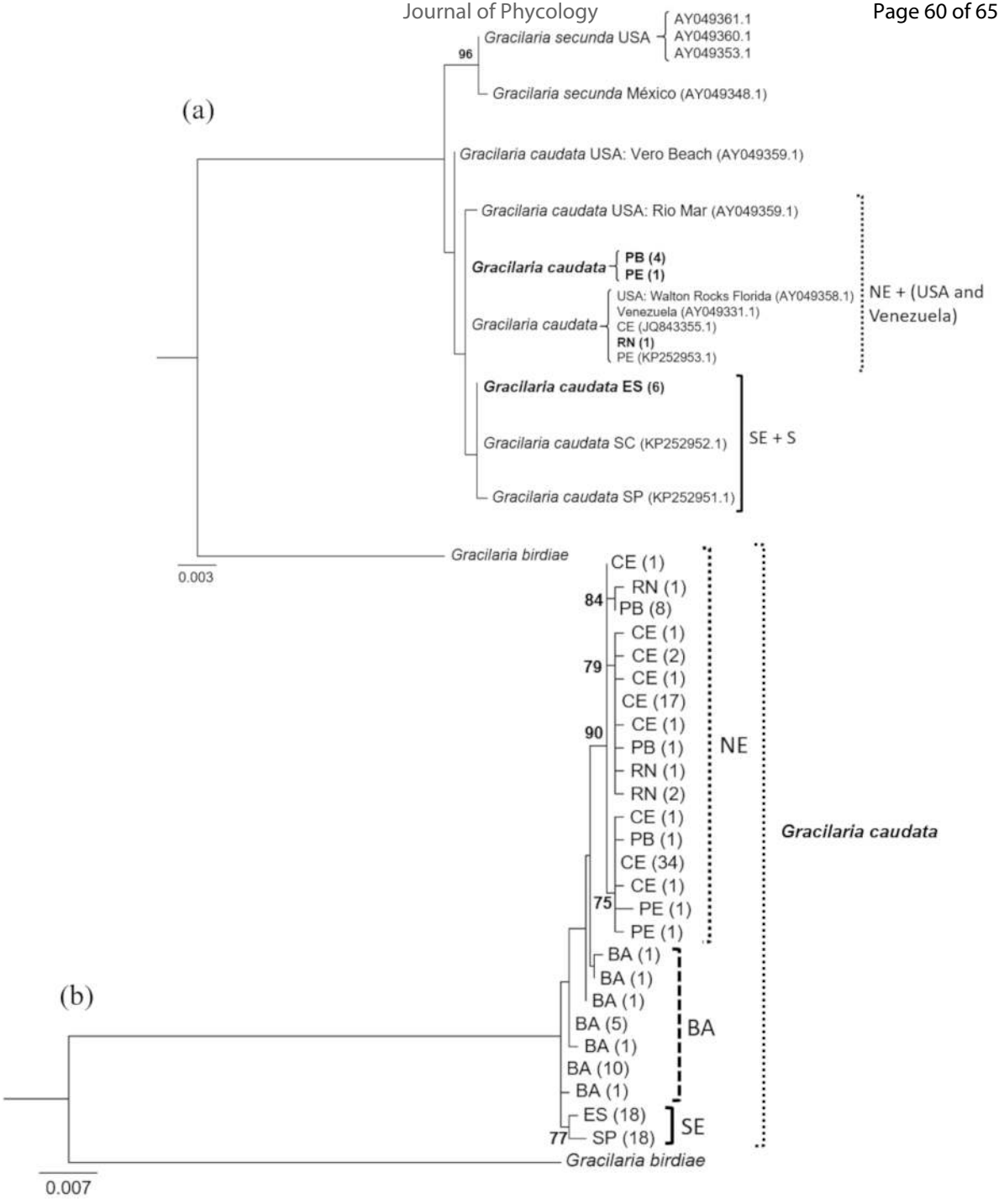
(a)
Gracilaria secunda USA
AY049361.1
AY049360.1
AY049353.1
96
Gracilaria secunda México (AY049348.1)
Gracilaria caudata USA: Vero Beach (AY049359.1)
Gracilaria caudata USA: Rio Mar (AY049359.1)
Gracilaria caudata
PB (4)
PE (1)
Gracilaria caudata
USA: Walton Rocks Florida (AY049358.1)
Venezuela (AY049331.1)
CE (JQ843355.1)
RN (1)
PE (KP252953.1)
NE + (USA and Venezuela)
Gracilaria caudata ES (6)
Gracilaria caudata SC (KP252952.1)
Gracilaria caudata SP (KP252951.1)
SE + S
Gracilaria birdiae
0.003
(b)
CE (1)
RN (1)
84
PB (8)
CE (1)
79
CE (2)
CE (1)
CE (17)
CE (1)
90
PB (1)
RN (1)
RN (2)
NE
CE (1)
PB (1)
CE (34)
CE (1)
75
PE (1)
PE (1)
Gracilaria caudata
BA (1)
BA (1)
BA (1)
BA (5)
BA (1)
BA
BA (10)
BA (1)
ES (18)
77
SP (18)
SE
Gracilaria birdiae
0.007

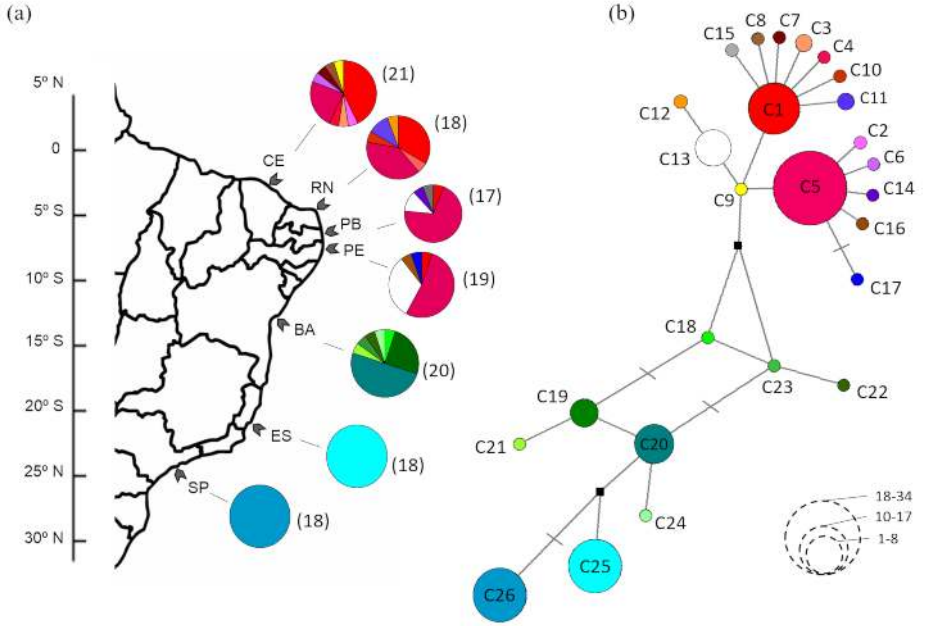
(a)
5° N
0
5° S
10° S
15° S
20° S
25° N
30° N
CE
RN
PB
PE
BA
ES
SP
(21)
(18)
(17)
(19)
(20)
(18)
(18)
(b)
C1
C2
C3
C4
C5
C6
C7
C8
C9
C10
C11
C12
C13
C14
C15
C16
C17
C18
C19
C20
C21
C22
C23
C24
C25
C26
18-34
10-17
1-8
(c)
K=2
K=3
NE
BA + SE
CE
RN
PB
PE
BA
ES
SP
K=3

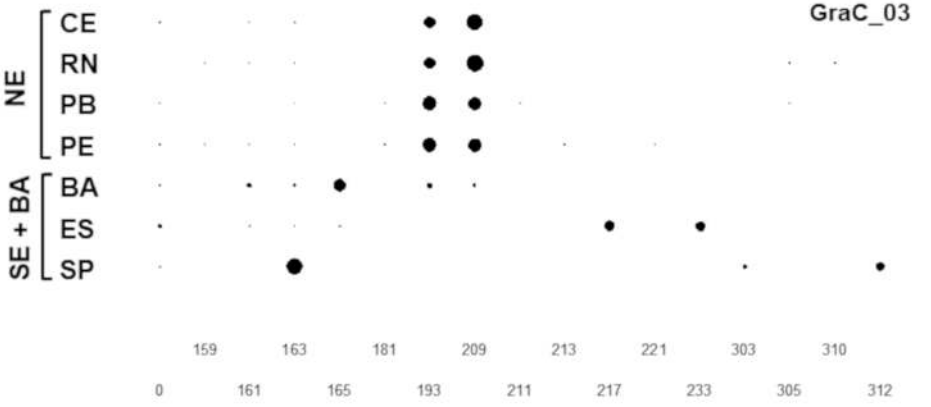
GraC_03
NE
CE
RN
PB
PE
SE + BA
BA
ES
SP
159
163
181
209
213
221
303
310
0
161
165
193
211
217
233
305
312

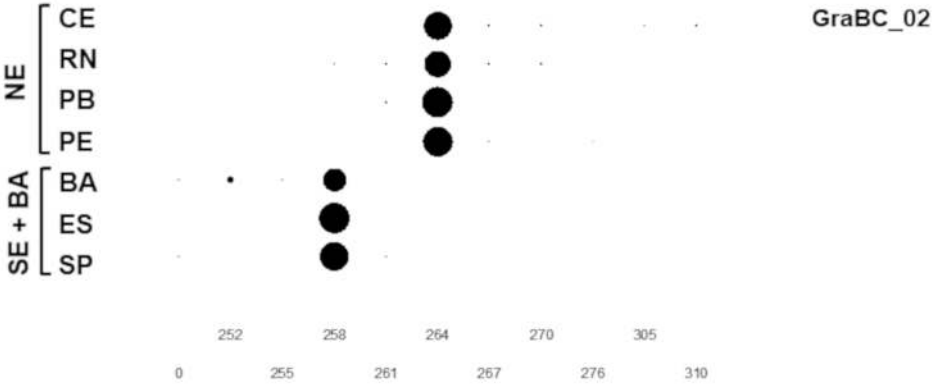
GraBC_02
NE
CE
RN
PB
PE
SE + BA
BA
ES
SP
252
258
264
270
305
0
255
261
267
276
310

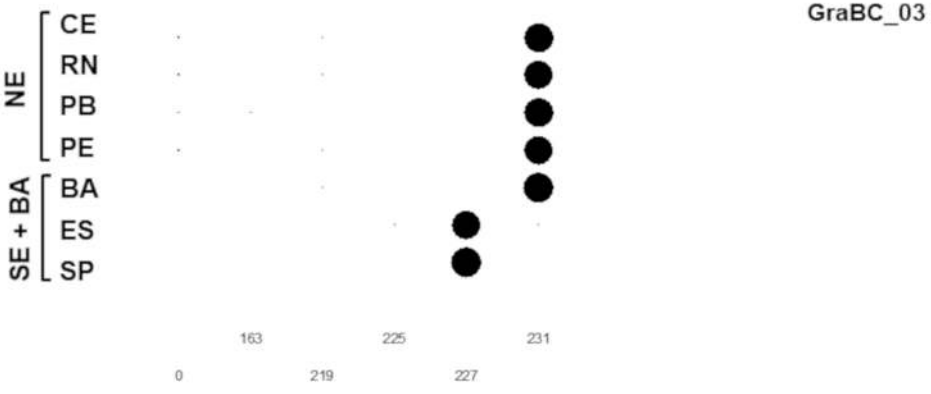
GraBC_03
NE
CE
RN
PB
PE
SE + BA
BA
ES
SP
163
225
231
0
219
227
Allele size

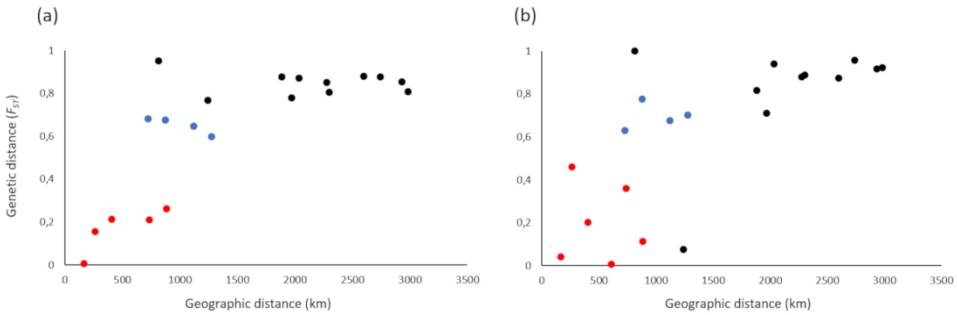

FIGURE S1 Mantel test of the relationship between genetic and geographic distances, using the mitochondrial markers (a) COI and (b) cox2-3, for the seven sampled Gracilaria caudata localities along the Brazilian coast, expressed as FST versus the distance in kilometres (km). The red dots represent relationship between genetic and geographic distances of among the north-east populations. The blue dots represent the relationship between genetic and geographic distances of the Bahia location and the remaining populations. The black dots represent relationship between genetic and geographic distances of among the south-east and the remaining populations.

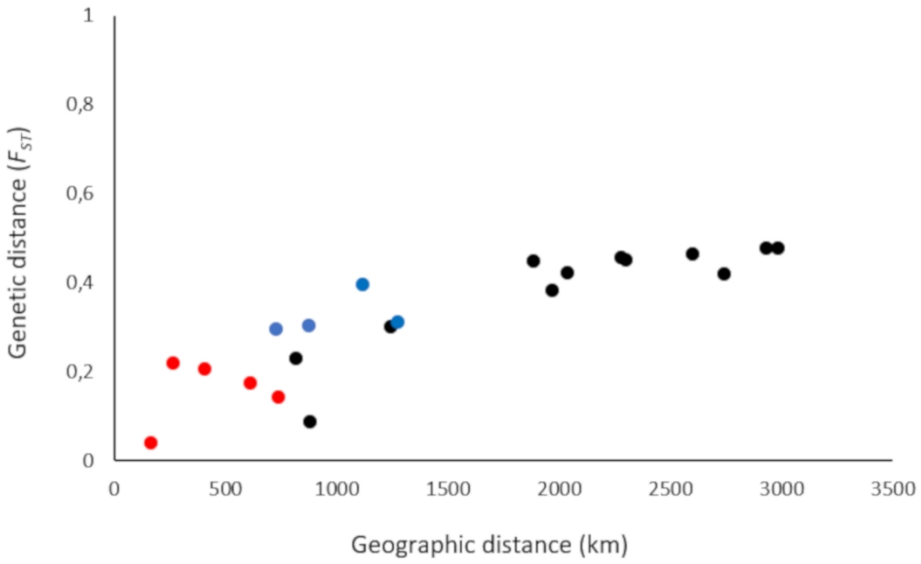

FIGURE S2 Mantel test of the relationship between genetic and geographic distance, using nuclear microsatellite markers, for the seven sampled Gracilaria caudata localities along the Brazilian coast, expressed as FST versus the distance in kilometres (km). The red dots represent relationship between genetic and geographic distances of among the north-east populations. The blue dots represent the relationship between genetic and geographic distances of the Bahia location and the remaining populations. The black dots represent relationship between genetic and geographic distances of among the south-east and the remaining populations.

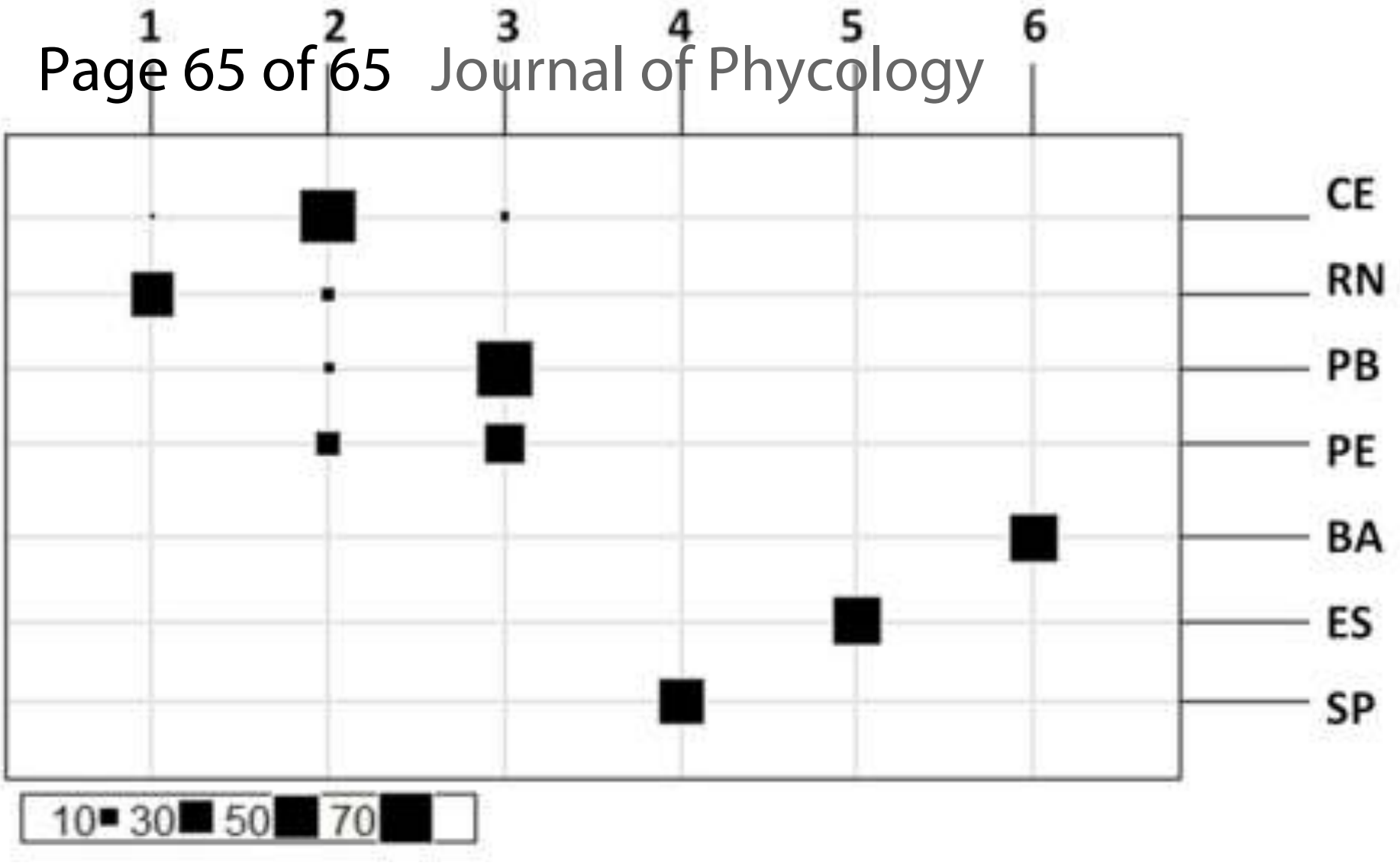
1
2
3
4
5
6
CE
RN
PB
PE
BA
ES
SP
10
30
50
70